

Classifying Complexity with the ZX-Calculus: Jones Polynomials and Potts Partition Functions

Alex Townsend-Teague^{0,1} and Konstantinos Meichanetzidis^{1,2}

⁰ Mathematical Institute, University of Oxford

¹ Department of Computer Science, University of Oxford

² Cambridge Quantum Computing Ltd.

The *ZX-calculus* is a graphical language which allows for reasoning about suitably represented tensor networks - namely *ZX-diagrams* - in terms of rewrite rules. Here, we focus on problems which amount to exactly computing a scalar encoded as a closed tensor network. In general, such problems are #P-hard. However, there are families of such problems which are known to be in P when the dimension is below a certain value. By expressing problem instances from these families as *ZX-diagrams*, we see that the easy instances belong to the stabilizer fragment of the *ZX-calculus*. Building on previous work on efficient simplification of qubit stabilizer diagrams, we present simplifying rewrites for the case of qutrits, which are of independent interest in the field of quantum circuit optimisation. Finally, we look at the specific examples of evaluating the Jones polynomial and of counting graph-colourings. Our exposition further champions the *ZX-calculus* as a suitable and unifying language for studying the complexity of a broad range of classical and quantum problems.

1 Introduction

A plethora of hard problems of interest to physics and computer science regard interacting many-body multi-state systems - both classical and quantum - and reduce to *exactly* computing a single scalar. These range from probability amplitudes in quantum mechanics, partition functions in classical statistical mechanics, counting problems, probabilistic inference, and many more. Problem instances can be encoded as closed tensor networks over an appropriate (semi)ring. The scalar can be evaluated by *full tensor contraction*, which in general is #P-hard [7]. In fact, finding the optimal contraction path for a general tensor network is NP-hard.

The *ZX-calculus* is a graphical language whose origin lies in the field of quantum foundations [6]. It allows for reasoning about *ZX-diagrams*, i.e. tensor networks which are expressed in terms of primitive generators [24]. The generators have a concrete representation as tensors over a (semi)ring and they obey a set of rewrite rules which respect semantics [23]. Importantly, the rewrite rules *depend* on the (semi)ring over which the diagram is interpreted as a tensor network. If a scalar of interest is expressed as a closed *ZX-diagram*, one can rewrite the diagram by applying rewrite rules; one's goal is then to perform *full diagram simplification* in order to compute the desired scalar. Again, simplifying arbitrary closed *ZX-diagrams* is #P-hard and finding the optimal rewrite strategy is NP-hard. Note that given an arbitrary tensor network, one can attempt to invent rewrite rules by inspecting the contents of the tensors and performing linear-algebra operations [13].

In the context of quantum computing, the Gottesman-Knill theorem states that stabilizer (or Clifford) circuits can be simulated *efficiently* on classical computers [1]. By simulation here we mean the *exact* computation of amplitudes. These circuits can be expressed by the *stabilizer* fragment of the *ZX-calculus*. An alternative - and in fact more general - proof of the Gottesman-Knill theorem for qubits

has been obtained graphically in terms of the qubit ZX-calculus. Interestingly, though the motivation for studying stabilizer diagrams stems from quantum computation, the result that stabilizer ZX-diagrams can be simplified efficiently has broader applicability. This is because ZX-diagrams can express arbitrary linear maps; every quantum circuit is a ZX-diagram but not vice versa.

Indeed, beyond quantum computing, ZX-diagrams have been leveraged to study the complexity of boolean satisfiability (SAT) and model counting (#SAT) [5]. Model counting entails computing the number of satisfying assignments to a boolean formula, and this number can be expressed as a closed diagram. Specifically, one finds that in the case of XORSAT and #XORSAT, which are known to be tractable, the corresponding ZX-diagrams representing the problems exactly correspond to qubit stabilizer diagrams, which are efficient to simplify. Going further, the ZH calculus [3], an extension of the ZX-calculus, can be imported to make graphically obvious why 2SAT is in P but #2SAT is #P-complete, whereas 3SAT and #3SAT are both hard. The key realisation is in that the decision problem is in fact a counting problem but where the diagram is interpreted over the Boolean semiring. Then the *rewrite rules change accordingly* and quickly imply the above result by allowing efficient simplification strategies.

Such observations make apparent the unifying power of diagrammatic reasoning for studying the complexity of problem families. Building on the spirit of [5], we treat the ZX-calculus as a library comprising out-of-the-box diagrammatic rewrite rules, from which we import the appropriate tools for the job depending on the occasion. The key rewrite rules that enable the efficient simplification of qubit stabilizer ZX-diagrams are called *local complementation* and *pivot*, the latter being a composition of three of the former [9]. In this work, we recall the *qutrit* version of local complementation and derive the corresponding pivot rule, which implies that qutrit stabilizer diagrams can be simplified *efficiently*. We then present two case studies: evaluating the Jones polynomial at lattice roots of unity, and graph colouring. Both of these problem families reduce to evaluating closed tensor networks and show a transition in complexity at a particular dimension, below which the tensor network corresponds to a stabilizer ZX-diagram.

We underline that throughout this work, all rewrites are valid *up to a scalar* since we are only concerned about making statements about complexity. Importantly, note that keeping track of multiplicative scalar factors that arise under diagram rewriting can be done efficiently. We are thus justified in omitting them for the purposes of this work. We also emphasise that the qutrit ‘elimination’ rewrite rules we derive in Section 3 have independent ramifications for circuit optimisation, though these are not explored here.

2 Simplifying Qubit ZX-Diagrams

In this section we briefly review the ZX-calculus, recalling the definitions of graph-like diagrams and stabilizer diagrams. Crucially, we also recall the simplifying rewrites that enable the efficient simplification of stabilizer diagrams.

2.1 The Qubit ZX-Calculus

Here we give a quick introduction to the qubit ZX-calculus. The qubit ZX-calculus is a diagrammatic language for quantum mechanics generated by *spiders*. The spider legs, or *wires*, represent vector spaces of dimension $d = 2$. Diagrams are read bottom-to-top; bottom open wires (not connected to anything) are *input wires* and top ones are *outputs*. Diagrams with only outputs are called *states* and those with only inputs are called *effects*. A *closed* diagram is one with no input nor output wires and it represents a

scalar.

Spiders can be *composed*; placing diagrams side by side represents parallel composition (\otimes), whose concrete interpretation is the tensor product. Vertically stacking diagrams corresponds to sequential composition (\circ) and concretely it means matrix multiplication. Specifically, it means tensor contraction of two spider tensors along the wires connecting them, i.e. the common tensor indices represented by these wires are summed over. The concrete representation of these operations of course depends on the (semi)ring over which the spiders are interpreted as tensors. For spiders S and S' , we denote these as

$$[[S \otimes S']] = [[S]] \otimes [[S']] \quad , \quad [[S \circ S']] = [[S]] \cdot [[S']] \quad (1)$$

Spiders come in two species: green Z-spiders and red X-spiders, decorated by a *phase* $\alpha \in [0, 2\pi)$. When $\alpha = 0$, we will omit it. The *standard representation* of the spider generators as tensors over \mathbb{C} is:

$$\left[\begin{array}{c} \overbrace{\quad}^m \\ \vdots \\ \text{green spider } \alpha \\ \vdots \\ \underbrace{\quad}_n \end{array} \right] = |0\rangle^{\otimes m} \langle 0|^{\otimes n} + e^{i\alpha} |1\rangle^{\otimes m} \langle 1|^{\otimes n} , \quad \left[\begin{array}{c} \overbrace{\quad}^m \\ \vdots \\ \text{red spider } \alpha \\ \vdots \\ \underbrace{\quad}_n \end{array} \right] = |+\rangle^{\otimes m} \langle +|^{\otimes n} + e^{i\alpha} |-\rangle^{\otimes m} \langle -|^{\otimes n} \quad (2)$$

where $\{|0\rangle, |1\rangle\}$ is the *Z-basis* and $|\pm\rangle = |0\rangle \pm |1\rangle$ the *X-basis* in \mathbb{C}^2 , in Dirac notation. The Hadamard gate H , whose function is to switch between the Z and X bases, is denoted as a yellow box. Often we will instead draw a dashed blue line to represent a *Hadamard edge*:

$$\begin{array}{c} | \\ \text{yellow box} \\ | \end{array} = \begin{array}{c} | \\ \text{dashed blue line} \\ | \end{array} = \begin{array}{c} \text{green } \frac{\pi}{2} \\ \text{red } \frac{\pi}{2} \\ \text{green } \frac{\pi}{2} \end{array} , \quad \left[\begin{array}{c} | \\ \text{yellow box} \\ | \end{array} \right] \simeq |0\rangle \langle 0| + |0\rangle \langle 1| + |1\rangle \langle 0| - |1\rangle \langle 1| \quad (3)$$

The ZX-calculus is universal for multilinear maps; any tensor over a (semi)ring has a corresponding ZX-diagram. The rewrite rules of the ZX-calculus (see Fig.1 in Appendix A) allow manipulation of the diagrams by *local tensor-rewrites*. Importantly, up to a scalar, the rewrites *preserve the semantics*, i.e. the concrete tensor representation over \mathbb{C} . The ZX-calculus is complete in the sense that any true equation between tensors can be proven *only* in terms of rewrites; the diagram on the left hand side of the equation can be transformed to that on the right hand side by applying rewrite rules. This gives ZX the status of a ‘calculus’. What is important about qubit ZX-diagrams is that *only topology matters*; the concrete tensor semantics of the diagram are invariant under deformations of the network as long as the inter-spider connectivity is respected.

2.2 Stabilizer Qubit ZX Diagrams

The *stabilizer fragment* of the calculus consists of all diagrams in which all phases are $\alpha = \frac{\pi n}{2}$, $n \in \mathbb{Z}$. In (Theorem 5.4, [9]) the authors give an efficient algorithm for simplifying any qubit ZX-diagram to an equivalent diagram with fewer spiders. The algorithm consists of consecutive applications of spider-eliminating rewrites.

First it is shown that every diagram is equivalent to a *graph-like* diagram: every spider is green, every edge is a Hadamard edge, there are no parallel edges or self-loops, every input and output wire

is connected to a spider and every spider has at most one input or output wire. The following derivable rules are key to this:

$$\begin{array}{c} \dots \\ \alpha \\ \dots \end{array} \text{ (loop) } = \begin{array}{c} \dots \\ \alpha \\ \dots \end{array}, \quad \begin{array}{c} \dots \\ \alpha \\ \dots \end{array} \text{ (loop) } = \begin{array}{c} \dots \\ \alpha \\ \dots \end{array}, \quad \begin{array}{c} \dots \\ \alpha \\ \dots \end{array} \text{ (loop) } = \begin{array}{c} \dots \\ \alpha + \pi \\ \dots \end{array} \quad (4)$$

Then the following two rewrite rules, derived via *local complementation* and *pivoting*, can be used to eliminate spiders:

$$\begin{array}{c} \alpha_1 \dots \alpha_n \\ \dots \end{array} \text{ (phase } \pm \frac{\pi}{2} \text{)} = \begin{array}{c} \alpha_1 \mp \frac{\pi}{2} \dots \alpha_n \mp \frac{\pi}{2} \\ \dots \end{array} \quad (5)$$

$$\begin{array}{c} \alpha_1 \dots \alpha_n \\ \dots \end{array} \text{ (phase } j\pi \text{)} \text{ --- } \begin{array}{c} \beta_1 \dots \beta_n \\ \dots \end{array} \text{ (phase } k\pi \text{)} = \begin{array}{c} \alpha_1 + k\pi \dots \alpha_n + k\pi \\ \dots \end{array} \text{ --- } \begin{array}{c} \beta_1 + (j+k+1)\pi \dots \beta_n + (j+k+1)\pi \\ \dots \end{array} \quad (6)$$

For more details, see (Section 4, [9]). Eq. (5) says that we can remove any spider with phase $\pm \frac{\pi}{2}$ at the cost of performing a local complementation at said spider. Furthermore, Eq. (6) says we can remove any pair of spiders with phases in $\{0, \pi\}$ connected by a Hadamard edge at the cost of performing a pivot along said edge. After each application of (5) or (6), we can use (4) to remove any parallel Hadamard edges and ensure the diagram remains graph-like.

In particular, and importantly to this work, this algorithm will *efficiently* simplify any closed stabilizer diagram until it contains at most one spider, at which point the scalar it represents can be easily read off. By ‘efficiently’ we mean via a sequence of spider elimination rewrites whose cost is polynomial in the initial number of spiders. Note each such rewrite updates only a polynomial number of edges in the diagram, which prevents an overwhelming memory cost of the simplification procedure.

3 Simplifying Qutrit ZX-Diagrams

We now turn to the qutrit ZX-calculus and examine the analogous story to that of the previous subsection, but now for the case where the dimension of the vector space carried by the wires is $d = 3$.

3.1 The Qutrit ZX-Calculus

As in the qubit case, the qutrit ZX-calculus concerns spiders connected by wires, but there are key differences, some subtler than others. Again, spiders come in two species, Z (green) and X (red), with the three-dimensional Z-basis denoted as $\{|0\rangle, |1\rangle, |2\rangle\}$. Let $\omega = e^{i\frac{2\pi}{3}}$ denote the third root of unity with $\bar{\omega} = \omega^2$ its complex conjugate. The qutrit X-basis consists of the three vectors:

$$|+\rangle = \frac{1}{\sqrt{3}}(|0\rangle + |1\rangle + |2\rangle), \quad |\omega\rangle = \frac{1}{\sqrt{3}}(|0\rangle + \omega|1\rangle + \bar{\omega}|2\rangle), \quad |\bar{\omega}\rangle = \frac{1}{\sqrt{3}}(|0\rangle + \bar{\omega}|1\rangle + \omega|2\rangle) \quad (7)$$

In the qutrit ZX-calculus, spiders carry *two* phases α and β , and have the following *standard representation* as linear maps:

$$\left[\begin{array}{c} \overbrace{\quad \quad \quad}^m \\ \vdots \\ \text{green spider } \alpha, \beta \\ \vdots \\ \underbrace{\quad \quad \quad}_n \end{array} \right] = |0\rangle^{\otimes m} \langle 0|^{\otimes n} + e^{i\alpha} |1\rangle^{\otimes m} \langle 1|^{\otimes n} + e^{i\beta} |2\rangle^{\otimes m} \langle 2|^{\otimes n} \quad (8)$$

$$\left[\begin{array}{c} \overbrace{\quad \quad \quad}^m \\ \vdots \\ \text{red spider } \alpha, \beta \\ \vdots \\ \underbrace{\quad \quad \quad}_n \end{array} \right] = |+\rangle^{\otimes m} \langle +|^{\otimes n} + e^{i\alpha} |\omega\rangle^{\otimes m} \langle \omega|^{\otimes n} + e^{i\beta} |\bar{\omega}\rangle^{\otimes m} \langle \bar{\omega}|^{\otimes n} \quad (9)$$

When $\alpha = \beta = 0$ we will again omit the angles entirely, and just draw a small green or red dot. Throughout our work, whenever we use an integer n as a spider decoration, this is a shorthand for $\frac{2\pi}{3}n$. Since spider phases hold mod 2π , these integer decorations hold mod 3. Unless otherwise stated, we will use Greek letters to denote general angles, and Roman letters for these integer shorthands.

Hadamard gates are no longer self-adjoint, so we change our notation: we let a yellow box decorated with a 1 (mod 3) denote a Hadamard gate, while decorating with a 2 (mod 3) denotes its adjoint. We will shortly explain this choice. We also use a dashed blue line for the *Hadamard edge* (H -edge) and a purple dashed line for its adjoint (H^\dagger -edge). Those familiar with the ZH-calculus should note that this notation is *not* analogous to the H-boxes therein.

$$\begin{array}{c} \text{yellow box } 1 \\ \hline \end{array} = \text{dashed blue line} = \begin{array}{c} \text{green spider } \frac{2}{2} \\ \hline \text{red spider } \frac{2}{2} \\ \hline \text{green spider } \frac{2}{2} \end{array}, \quad \begin{array}{c} \text{yellow box } 2 \\ \hline \end{array} = \text{dashed purple line} = \begin{array}{c} \text{green spider } \frac{1}{1} \\ \hline \text{red spider } \frac{1}{1} \\ \hline \text{green spider } \frac{1}{1} \end{array}, \quad \begin{array}{c} \text{yellow box } 0 \\ \hline \end{array} = \text{two green dots} \quad (10)$$

The last equation above says that in a graph-like diagram (which we will define shortly), a Hadamard edge decorated by a 0 is in fact not an edge at all, thanks to spider fusion. A very important difference from the qubit case is that in qutrit ZX-calculus there is no *plain* cap or cup:

$$\begin{array}{c} \text{green cap} \end{array} \neq \begin{array}{c} \text{red cap} \end{array}, \quad \begin{array}{c} \text{green cup} \end{array} \neq \begin{array}{c} \text{red cup} \end{array} \quad (11)$$

This has several consequences. Firstly, the maxim that ‘*only topology matters*’ *no longer applies*. That is, it is now important to make clear the distinction between a spider’s input and output wires, unlike in the qubit case where we could freely interchange the two. Diagram components can still be isotoped around the plane but only so long as this input/output distinction is respected. This gives the qutrit calculus a slightly more rigid flavour than its qubit counterpart. That said, this rigidity is loosened in certain cases; in particular, this distinction is irrelevant for H - and H^\dagger -edges [11]:

$$\begin{array}{c} \text{green spider } \alpha, \beta \\ \text{dashed blue line} \\ \text{green spider } \gamma, \delta \end{array} = \begin{array}{c} \text{green spider } \alpha, \beta \\ \text{dashed blue line} \\ \text{red spider } \gamma, \delta \end{array}, \quad \begin{array}{c} \text{green spider } \alpha, \beta \\ \text{dashed purple line} \\ \text{green spider } \gamma, \delta \end{array} = \begin{array}{c} \text{green spider } \alpha, \beta \\ \text{dashed purple line} \\ \text{red spider } \gamma, \delta \end{array} \quad (12)$$

The full set of rules governing the qutrit ZX-calculus is shown in Figure 2 in Appendix A.

3.2 Graph-Like Qutrit ZX Diagrams

A *graph-like* qutrit ZX-diagram is one where every spider is green, spiders are only connected by blue Hadamard edges (H -edges) or their purple adjoints (H^\dagger -edges), every pair of spiders is connected by at most one H -edge or H^\dagger -edge, every input and output wire is connected to a spider, and every spider is connected to at most one input or output wire. A graph-like qutrit ZX-diagram is a *graph state* when every spider has zero phase (top and bottom) and is connected to an output.

Note the difference compared to the qubit case: we need not worry about self-loops because the qutrit ZX-calculus doesn't define a 'plain' cap or cup. But this comes at a cost: spiders in the qutrit case fuse more fussily. Specifically, when two spiders of the same colour are connected by at least one plain edge and at least one H - or H^\dagger -edge, fusion is not possible. Instead, should we want to ensure we have a graph-like diagram, we can replace the plain wire:

$$\begin{array}{c} | \\ \text{(H)} \\ \text{(id)} \end{array} = \begin{array}{c} \text{2} \\ \text{1} \end{array} = \begin{array}{c} \text{2} \\ \text{1} \end{array} = \begin{array}{c} \text{2} \\ \text{1} \end{array} = \begin{array}{c} \text{2} \\ \text{1} \end{array} \quad (13)$$

Indeed, we can show that every qutrit ZX-diagram is equivalent to a graph-like one. The following equations, derived in Appendix B.3, are vital to this:

$$\begin{array}{c} \dots \\ \alpha \\ \beta \\ \gamma \\ \delta \\ \dots \end{array} = \begin{array}{c} \dots \\ \alpha \\ \beta \\ \gamma \\ \delta \\ \dots \end{array} = \begin{array}{c} \dots \\ \alpha \\ \beta \\ \gamma \\ \delta \\ \dots \end{array}, \quad \begin{array}{c} \dots \\ \alpha \\ \beta \\ \gamma \\ \delta \\ \dots \end{array} = \begin{array}{c} \dots \\ \alpha \\ \beta \\ \gamma \\ \delta \\ \dots \end{array}, \quad \begin{array}{c} \dots \\ \alpha \\ \beta \\ \gamma \\ \delta \\ \dots \end{array} = \begin{array}{c} \dots \\ \alpha \\ \beta \\ \gamma \\ \delta \\ \dots \end{array} \quad (14)$$

This justifies our notation for Hadamard gates: we can think of Hadamard edges as 1-weighted edges and their adjoints as 2-weighted edges, then work modulo 3, since every triple of parallel edges disappears. Where the previous equations relate single H - and H^\dagger -boxes across multiple edges, the next three relate multiple H - and H^\dagger -boxes on single edges. They hold for $h \in \{1, 2\}$, and are proved via simple applications of rules (id), (H) and (s).

$$\begin{array}{c} h \\ h \\ h \\ h \end{array} = \begin{array}{c} | \\ \text{---} \\ | \end{array}, \quad \begin{array}{c} h \\ h \\ h \\ h \end{array} = \begin{array}{c} h \\ \text{---} \\ h \end{array}, \quad \begin{array}{c} h \\ h \end{array} = \begin{array}{c} h \\ \text{---} \\ h \end{array} \quad (15)$$

Proposition 3.1. Every qutrit ZX-diagram is equivalent to one that is graph-like.

Proof. First use the colour change rule to turn all X -spiders into Z -spiders. Then use (15) to remove excess H - and H^\dagger -boxes, inserting a spider between any remaining consecutive pair of such boxes, so that all spiders are connected only by plain edges, H -edges or H^\dagger -edges. Fuse together as many as possible, and apply (13) where fusion is not possible, so that no plain edge connects two spiders. Apply (14) to all connected pairs of spiders until at most one H - or H^\dagger -edge remains between them. Finally, to

ensure every input and output is connected to a spider and every spider is connected to at most one input or output, we can use **(H)** and **(id)** to add a few spiders, H - and H^\dagger -edges as needed:

$$\begin{array}{c} | \end{array} = \begin{array}{c} \text{green circle} \\ \vdots \\ \text{green circle} \end{array}, \quad \begin{array}{c} | \end{array} = \begin{array}{c} \text{yellow box } h \\ \vdots \\ \text{green circle} \end{array}, \quad \begin{array}{c} \dots \\ \text{green circle} \\ \dots \end{array} = \begin{array}{c} \dots \\ \text{green circle} \\ \dots \end{array} \quad (16)$$

□

A graph state is described fully by its underlying multigraph, or equivalently by an adjacency matrix, where edges take weights in \mathbb{Z}_3 (Lemma 4.2, [22]). Nodes correspond to phaseless green spiders, edges of weight 1 correspond to Hadamard edges, and edges of weight 2 correspond to H^\dagger -edges. As in the qubit case, graph states admit a *local complementation* operation (Definition 2.6, [22]), though the effect is now slightly more complicated. We'll give the intuition after the formal definition:

Definition 3.2. Given $a \in \mathbb{Z}_3$ and a graph state G with adjacency matrix $W = (w_{i,j})$, the a -local complementation at node x is the new graph state $G *_a x$, whose adjacency matrix $W' = (w'_{i,j})$ is given by $w'_{i,j} = w_{i,j} + aw_{i,x}w_{j,x}$.

So only those edges between neighbours of node x are affected. Specifically, for two nodes i and j both connected to x by the *same* colour edge, a -local complementation at x *increases* weight $w_{i,j}$ by a . If instead i and j are connected to x by edges of *different* colours, a -local complementation at x *decreases* $w_{i,j}$ by a . This is shown graphically below, and holds with the roles of blue and purple interchanged:

$$\begin{array}{c} \text{blue} \quad \text{blue} \\ \text{green} \quad \text{green} \end{array} \xrightarrow{*a} \begin{array}{c} \text{blue} \quad \text{blue} \\ \text{green} \quad \text{green} \end{array}, \quad \begin{array}{c} \text{blue} \quad \text{purple} \\ \text{green} \quad \text{green} \end{array} \xrightarrow{*a} \begin{array}{c} \text{blue} \quad \text{purple} \\ \text{green} \quad \text{green} \end{array} \quad (17)$$

Theorem 3.3. (Theorem 4.4, Corollary 4.5, [22]) Given $a \in \mathbb{Z}_3$ and a graph state (G, W) containing a node x , let $N(x)$ denote the neighbours of x ; that is, nodes i with weight $w_{i,x} \in \{1, 2\}$. Then the following equality holds:

$$\begin{array}{c} x \\ \text{green circle} \\ \vdots \\ \text{green circle} \end{array} \xrightarrow{*a} \begin{array}{c} x \\ \text{red circle} \\ \vdots \\ \text{green circle} \end{array} \quad (18)$$

Definition 3.4. Given $a, b, c \in \mathbb{Z}_3$ and a graph state G containing nodes i and j , the (a, b, c) -pivot along ij is the new graph state $G \wedge_{(a,b,c)} ij := ((G *_a i) *_b j) *_c i$.

This pivot operation again leads to an equality, up to introducing some extra gates on outputs, whose proof is found in Appendix C.1. Here we shall only consider an $(a, -a, a)$ -pivot along an edge ij of non-zero weight, for $a \in \{1, 2\}$. We will call this a *proper a -pivot* along ij , and denote it $G \wedge_a ij$.

Theorem 3.5. Given $a \in \mathbb{Z}_3$ and a graph state (G, W) containing connected nodes i and j , define $N_=(i, j) := \{x \in N(i) \cap N(j) \mid w_{x,i} = w_{x,j}\}$ and $N_\neq(i, j) := \{x \in N(i) \cap N(j) \mid w_{x,i} \neq w_{x,j}\}$. Then the following equation relates G and its proper a -pivot along ij :

$$\begin{array}{c} i \quad j \\ \text{green circle} \quad \text{green circle} \end{array} \xrightarrow{\wedge_a} \begin{array}{c} i \quad j \\ \text{yellow box } -a \quad \text{yellow box } a \end{array} \quad (19)$$

3.3 Qutrit Elimination Theorems

We classify spiders into three families exactly as in (Theorem 3.1, [22]):

$$\mathcal{M} = \left\{ \begin{array}{c} \cdots \\ \textcircled{0} \\ \cdots \end{array}, \begin{array}{c} \cdots \\ \textcircled{1} \\ \cdots \end{array}, \begin{array}{c} \cdots \\ \textcircled{2} \\ \cdots \end{array} \right\}, \quad \mathcal{N} = \left\{ \begin{array}{c} \cdots \\ \textcircled{0} \\ \cdots \end{array}, \begin{array}{c} \cdots \\ \textcircled{1} \\ \cdots \end{array}, \begin{array}{c} \cdots \\ \textcircled{2} \\ \cdots \end{array}, \begin{array}{c} \cdots \\ \textcircled{2} \\ \cdots \end{array} \right\}, \quad \mathcal{P} = \left\{ \begin{array}{c} \cdots \\ \textcircled{1} \\ \cdots \end{array}, \begin{array}{c} \cdots \\ \textcircled{2} \\ \cdots \end{array} \right\} \quad (20)$$

We call a spider in a graph-like ZX-diagram *interior* if it isn't connected to an input or output. Given any graph-like ZX-diagram, we will show that we can eliminate standalone interior \mathcal{P} - and \mathcal{N} -spiders by local complementation, and pairs of connected interior \mathcal{M} -spiders by pivoting.

First, we define (a very small extension of) the *!-box* notation (pronounced 'bang-box'), as introduced in [8] for general string diagrams. A *!-box* in a ZX-diagram is a compressed notation for a family of diagrams; the contents of the *!-box*, along with any wires into or out of it, are 'unfolded' (copied) $n \geq 0$ times and placed side-by-side. Following the style of [3], we also allow a parameter over which a *!-box* unfolds. We extend this notation as follows: in the top-left corner of the *!-box* we introduce a further diagram, which denotes that the spiders unfolded by the *!-box* have a complete graph imposed on them, whose edges take the form of this 'corner diagram'. In qutrit ZX-diagrams this notation will only be well-defined in certain scenarios: in particular, it is well-defined when the corner diagram is a H - or H^\dagger -edge (since then the distinction between a spider's input and output wires disappears) and the main contents of the *!-box* is equivalent to a single spider (since then there is no ambiguity about which spiders are connected by the corner diagram). For example, letting $[K] = \{1, \dots, K\}$, we have:

$$\left\{ \begin{array}{c} k \in [K] \\ \textcircled{\alpha_k} \\ \beta_k \end{array} : K \in \{0, 1, 2, 3, 4, \dots\} \right\} = \left\{ \begin{array}{c} \text{diagram 1} \\ \text{diagram 2} \\ \text{diagram 3} \\ \text{diagram 4} \\ \text{diagram 5} \\ \dots \end{array} \right\}$$

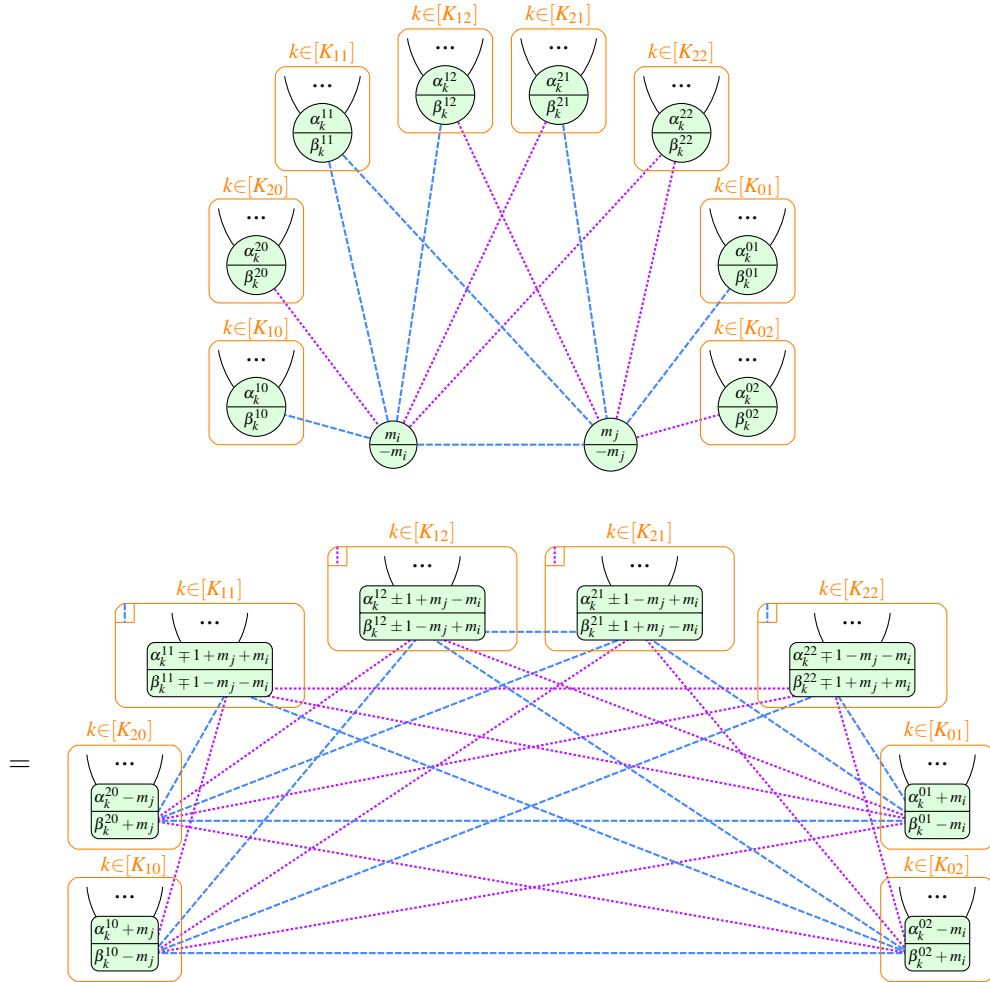
Theorem 3.6. Given any graph-like ZX-diagram containing an interior \mathcal{P} -spider x with phase $\textcircled{\frac{p}{p}}$ for $p \in \{1, 2\}$, suppose we perform a p -local complementation at x . Then the new ZX-diagram is related to the old one by the following equality:

$$\begin{array}{c} k \in [K_1] \quad k \in [K_2] \\ \textcircled{\alpha_k} \quad \textcircled{\gamma_k} \\ \beta_k \quad \delta_k \\ \textcircled{\frac{p}{p}} \end{array} = \begin{array}{c} k \in [K_1] \quad k \in [K_2] \\ \textcircled{\alpha_k - p} \quad \textcircled{\gamma_k - p} \\ \beta_k - p \quad \delta_k - p \\ \textcircled{-p} \end{array}$$

Theorem 3.7. Given any graph-like ZX-diagram containing an interior \mathcal{N} -spider x with phase $\textcircled{\frac{0}{n}}$ or $\textcircled{\frac{n}{0}}$ for $n \in \{1, 2\}$, suppose we perform a $(-n)$ -local complementation at x . Then, treating the two cases separately, the new ZX-diagrams are related to the old ones by the equalities:

$$\begin{array}{c} k \in [K_1] \quad k \in [K_2] \\ \textcircled{\alpha_k} \quad \textcircled{\gamma_k} \\ \beta_k \quad \delta_k \\ \textcircled{\frac{0}{n}} \end{array} = \begin{array}{c} k \in [K_1] \quad k \in [K_2] \\ \textcircled{\alpha_k + n + 2} \quad \textcircled{\gamma_k + n + 1} \\ \beta_k + n + 1 \quad \delta_k + n + 2 \\ \textcircled{n} \end{array}, \quad \begin{array}{c} k \in [K_1] \quad k \in [K_2] \\ \textcircled{\alpha_k} \quad \textcircled{\gamma_k} \\ \beta_k \quad \delta_k \\ \textcircled{\frac{n}{0}} \end{array} = \begin{array}{c} k \in [K_1] \quad k \in [K_2] \\ \textcircled{\alpha_k + n + 1} \quad \textcircled{\gamma_k + n + 2} \\ \beta_k + n + 2 \quad \delta_k + n + 1 \\ \textcircled{-n} \end{array}$$

Theorem 3.8. Given any graph-like ZX-diagram containing two interior \mathcal{M} -spiders i and j connected by edge ij of weight $w_{i,j} =: w \in \{1, 2\}$, suppose we perform a proper $\pm w$ -pivot along ij (both choices give the same result). For the case $w = 1$, the new ZX-diagram is related to the old one by the following equality:



The case $w = 2$ differs only as follows: in the first diagram (the left hand side of the equation), the edge ij is purple (by definition), while in the lower diagram (the right hand side of the equation), a $\pm 2 = \mp 1$ will replace all occurrences of ± 1 , and the roles of purple and blue will be swapped throughout.

Proofs of these theorems are found in Appendix D.4, D.7 and D.8 respectively. We can now combine them into an algorithm for efficiently simplifying a *closed* graph-like ZX-diagram. First note that after applying any one of the three elimination theorems to such a diagram, and perhaps removing parallel H - or H^\dagger -edges via (14), we again have a graph-like diagram.

Theorem 3.9. Given any closed graph-like ZX-diagram, the following algorithm will always terminate after a finite number of steps, returning an equivalent graph-like ZX-diagram with no \mathcal{N} -spiders, \mathcal{P} -spiders, or adjacent pairs of \mathcal{M} -spiders. Repeat the steps below until no rule matches. After each step, apply (14) as needed until the resulting diagram is graph-like:

1. Eliminate a \mathcal{P} -spider via Theorem 3.6.
2. Eliminate an \mathcal{N} -spider via Theorem 3.7.

3. Eliminate two adjacent \mathcal{M} -spiders via Theorem 3.8.

Proof. At every step the total number of spiders decreases by at least one, so since we start with a finite diagram the algorithm terminates after a finite number of steps. By construction, when it does so we are left with an equivalent graph-like ZX-diagram with no \mathcal{N} -spiders, \mathcal{P} -spiders, or adjacent pairs of \mathcal{M} -spiders. \square

In particular, if we start with a stabilizer diagram, we can eliminate all but perhaps one spider, depending on whether the initial number of \mathcal{M} -spiders was odd or even. This is because no step introduces any non-stabilizer phases. The algorithm above could be extended to a *non-closed* graph-like diagrams as in (Theorem 5.4, [9]) - for example, as part of a qutrit circuit optimisation algorithm. However, since this paper focuses on using the ZX-calculus to simplify *closed* tensor networks, we have not done so.

4 Case studies

In this section we present two problems which can naturally be cast in tensor network form. These problem families are interesting in that they show a transition in complexity when the dimension d carried by the wires of the network is greater than a specific value. The *Jones polynomial* is a prominent *link invariant* in knot theory; here we present the problem of evaluating it at the *lattice roots of unity*. Subsequently, we briefly look at graph colouring.

4.1 Jones Polynomial at Lattice Roots of Unity

A *knot* K is a circle embedded in \mathbb{R}^3 . A set of knots tangled together make a *link* L . A link L can be represented by a *link diagram* by projecting it on to the plane but retaining the information of *over or under crossings*. We say that $L \simeq L'$ iff the diagram of link L can be deformed to that of link L' without cutting or gluing strands, or passing strands through each other. The Jones polynomial $V_L(t)$ is a Laurent polynomial in a variable $t \in \mathbb{C}$ and is a *link invariant*. This means that $V_L(t) \neq V_{L'}(t) \Rightarrow L \not\simeq L'$.

In general, computing $V_L(t)$ is exponentially costly in the number of crossings c , something made explicit when one uses the Kauffman bracket method [16]. Exactly evaluating the Jones polynomial at points $t \in \mathbb{C}$ is #P-hard, *except* at the *lattice roots of unity* $\Lambda = \{\pm 1, \pm i, \pm e^{i2\pi/3}, \pm e^{i4\pi/3}\}$, where it can be evaluated at cost $O(\text{poly}(c))$ [15].

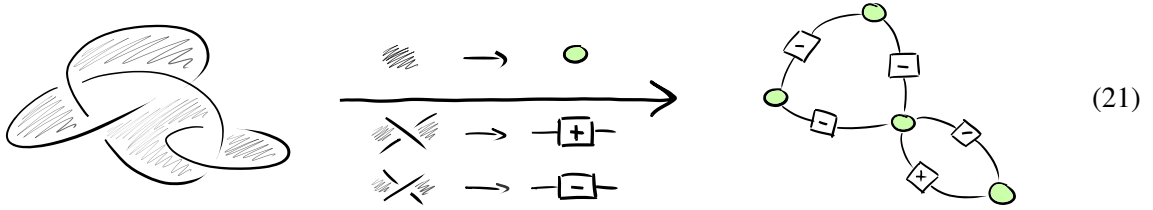
In the context of quantum computation, additively approximating the Jones polynomial at *non-lattice roots of unity* is the paradigmatic BQP-complete problem [2, 17]. Topological quantum computation [10, 20] is the most natural model for such knot theoretic questions. In this model, quantum states are defined in the fusion space of *non-abelian anyons*, emergent quasiparticles with nontrivial exchange statistics arising in two-dimensional exotic phases of matter. Quantum computation is performed by creating anyons from the vacuum, then braiding them, and finally fusing them back to the vacuum, where braids play the role of unitary gates. The world-lines of the anyons define a closed braid, i.e. a link. Such a link encodes a quantum amplitude corresponding to its Jones polynomial evaluated at a root of unity depending on the anyon theory at hand [25]. Specifically, in the case of $SU(2)_k$ anyons, the Jones polynomial is evaluated at $t(k) = e^{i2\pi/(2+k)}$ [21].

Remarkably, the evaluation of the Jones polynomial at certain points can be expressed as an unphysical partition function $Z_{G_L}(d)$ of a d -state Potts model with suitable spin-spin interactions [26]. This Potts model is defined on a signed graph G_L , obtained as follows. The link diagram is bicoloured checkerboard-style, then every coloured area is mapped to a vertex and every crossing is mapped to a

signed edge according to its orientation relative to the surrounding colours, as in (21) below. The Jones polynomial is then equal to this partition function up to an efficiently computable scalar which depends on the link diagram. The relation between the point $t(d)$ at which the Jones polynomial is evaluated and the dimension d of the spins is $d = t + t^{-1} + 2$, which can be solved for $t(d)$ [19].

Note the correspondence between the dimension d in the Potts approach and the level k in the anyon-braiding approach to the Jones polynomial: $\{t(d) \mid d \in \{1, 2, 3, 4\}\} = \{t(k) \mid k \in \{1, 2, 4, \infty\}\} \subseteq \Lambda$. This is consistent with the fact that braiding $SU(2)_2$ anyons (Ising) or $SU(2)_4$ anyons is not universal (unless the $SU(2)_4$ anyons are augmented by fusion and measurements [18]).

The partition function $Z_{G_L}(d \in \mathbb{N})$ can be expressed as a closed tensor network in terms of phaseless (green) d -dimensional Z -spiders connected via wires that go through \pm -boxes [19]:



The \pm -boxes have the following concrete interpretation as matrices:

$$\left[\begin{array}{c} \pm \\ \hline \end{array} \right] = \sum_{i,j=0}^{d-1} (1 - (1 + t(d)^{\mp 1}) \delta_{ij}) |i\rangle \langle j| = \begin{pmatrix} -t(d)^{\mp 1} & 1 & \dots & 1 \\ 1 & -t(d)^{\mp 1} & \dots & 1 \\ \vdots & \vdots & \ddots & \vdots \\ 1 & 1 & \dots & -t(d)^{\mp 1} \end{pmatrix} \quad (22)$$

We can now express the \pm -boxes in the ZX-calculus. The \pm -matrices above for $d \in \{2, 4\}$ are equal up to a scalar to concrete interpretations of *qubit stabilizer* ZX-diagrams, and the \pm -matrices for $d = 3$ of *qutrit stabilizer* ZX-diagrams (see Appendix E.1):

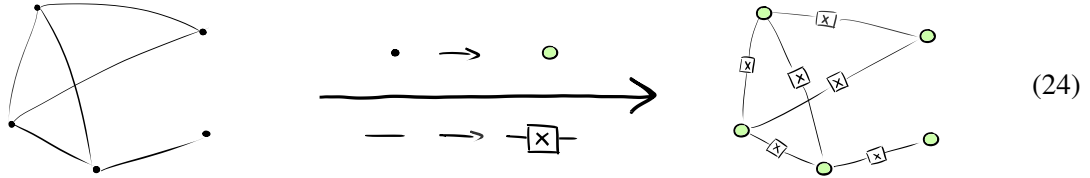
$$\left[\begin{array}{c} \pm \\ \hline \end{array} \right]_{d=2} \simeq \left[\begin{array}{c} \pm \frac{\pi}{2} \\ \hline \end{array} \right], \quad \left[\begin{array}{c} \pm \\ \hline \end{array} \right]_{d=3} \simeq \left[\begin{array}{c} \pm 1 \\ \pm 1 \\ \pm 1 \\ \hline \end{array} \right], \quad \left[\begin{array}{c} \pm \\ \hline \end{array} \right]_{d=4} \simeq \left[\begin{array}{c} \pi \\ \hline \end{array} \right] \text{---} \left[\begin{array}{c} \pi \\ \hline \end{array} \right] \quad (23)$$

Since these generators decompose as stabilizer diagrams, $Z_{G_L}(d \in \{2, 3, 4\})$ can be evaluated *efficiently* via stabilizer ZX-diagram simplification. Thus, we recover the known result that evaluating the Jones polynomial at $t \in \Lambda$ is in P. Computing $Z_{G_L}(d \geq 5)$ is #P-hard.

4.2 Graph Colouring

Finally, let us briefly look at the *graph colouring problem*. A d -colouring of a graph G is an assignment of colours $\{1, \dots, d\}$ to the vertices of G so that no neighbouring vertices have the same colour. Given a graph G and an integer d , we wish to *count* the number of such d -colourings. Again, this problem can be interpreted as the zero-temperature partition function of an antiferromagnetic Potts model (there is an energy cost for adjacent spins to be in the same state). Through the lens of our graphical exposition we see that counting problems and computing partition functions are essentially the same problem, since both can be straightforwardly encoded as closed tensor networks.

Given a graph G , the graph colouring problem can be encoded as a ZX-diagram as follows. Every vertex of the graph is mapped to a d -dimensional phaseless (green) Z-spider. Every edge is mapped to a wire connecting the spiders which goes through an X -box.



The X -boxes have the following concrete interpretation (as special case of the \pm -boxes, where $t = 0$):

$$\left[\begin{array}{c} | \\ \boxed{X} \\ | \end{array} \right] = \sum_{i,j=0}^{d-1} (1 - \delta_{ij}) |i\rangle \langle j| = \begin{pmatrix} 0 & 1 & \dots & 1 \\ 1 & 0 & \dots & 1 \\ \vdots & \vdots & \ddots & \vdots \\ 1 & 1 & \dots & 0 \end{pmatrix} \quad (25)$$

Counting k -colourings for $k \geq 3$ is a canonical $\#P$ -complete problem, while for $k = 0, 1, 2$ the problem is in P [15]. And indeed, for $d = 2$ the X -matrix is just the Pauli X , and so the problem reduces to simplifying a stabilizer diagram, which can be done efficiently.

$$\left[\begin{array}{c} | \\ \boxed{X} \\ | \end{array} \right]_{d=2} \simeq \left[\begin{array}{c} | \\ \textcircled{\pm\pi} \\ | \end{array} \right] \quad (26)$$

However, for $d = 3$ the X -matrix cannot be expressed as a stabilizer qutrit diagram; any such diagram must be unitary [14], but the X -matrix is not. Thus it is not expected that there exists an efficient simplification strategy for the corresponding qutrit ZX-diagram. This is consistent with the fact that counting 3-colourings is $\#P$ -complete. a

5 Outlook

In this work, we have advocated for the use of the ZX-calculus as a convenient graphical framework for treating a broad range of many-body problems on equal footing, and for diagnosing the complexity of interesting families of problems. When the solution to a problem is encoded as a closed ZX-diagram, this solution can be obtained via full diagram simplification by applying the rules of the calculus. The problem can be solved *efficiently* when the diagram encoding its answer is in the stabilizer fragment of the calculus. In this work specifically, we have fleshed out the simplifications strategies that make this apparent for the case of qutrits.

We also looked at two case studies. We reviewed complexity results on evaluating the Jones polynomial and counting graph colourings, two problems which can be cast in tensor network form. We then recovered known complexity results using only the language of the ZX-calculus.

A main path for future work entails the generalisation of our stabilizer simplification rules to all prime dimensions. This in turn also motivates work in circuit extraction [4] for qudit circuits; one could hope to find graph-theoretic simplification [9] strategies analogous to those for the case of qubits. Another direction regards defining scalar-exact versions of the rewrite rules, which would be necessary for concrete applications to problems where d -state systems are the native degrees of freedom.

6 Acknowledgments

We wish to thank Niel de Beaudrap, Aleks Kissinger, Stefanos Kourtis, and Quanlong (Harny) Wang for inspiring and helpful discussions. KM acknowledges financial support from the Royal Commission for the Exhibition of 1851 through a postdoctoral research fellowship.

References

- [1] Scott Aaronson & Daniel Gottesman (2004): *Improved simulation of stabilizer circuits*. *Physical Review A* 70(5), doi:10.1103/physreva.70.052328. Available at <http://dx.doi.org/10.1103/PhysRevA.70.052328>.
- [2] Dorit Aharonov, Vaughan Jones & Zeph Landau (2008): *A Polynomial Quantum Algorithm for Approximating the Jones Polynomial*. *Algorithmica* 55(3), p. 395–421, doi:10.1007/s00453-008-9168-0. Available at <http://dx.doi.org/10.1007/s00453-008-9168-0>.
- [3] Miriam Backens & Aleks Kissinger (2018): *ZH: A Complete Graphical Calculus for Quantum Computations Involving Classical Non-linearity*.
- [4] Miriam Backens, Hector Miller-Bakewell, Giovanni de Felice, Leo Lobski & John van de Wetering (2020): *There and back again: A circuit extraction tale*.
- [5] Niel de Beaudrap, Aleks Kissinger & Konstantinos Meichanetzidis (2020): *Tensor Network Rewriting Strategies for Satisfiability and Counting*.
- [6] Bob Coecke & Ross Duncan (2011): *Interacting quantum observables: categorical algebra and diagrammatics*. *New Journal of Physics* 13(4), p. 043016, doi:10.1088/1367-2630/13/4/043016. Available at <http://dx.doi.org/10.1088/1367-2630/13/4/043016>.
- [7] Carsten Damm, Markus Holzer & Pierre McKenzie (2002): *The complexity of tensor calculus*. *computational complexity* 11(1), pp. 54–89, doi:10.1007/s00037-000-0170-4. Available at <https://doi.org/10.1007/s00037-000-0170-4>.
- [8] Lucas Dixon & Ross Duncan (2009): *Graphical reasoning in compact closed categories for quantum computation*. *Annals of Mathematics and Artificial Intelligence* 56(1), pp. 23–42.
- [9] Ross Duncan, Aleks Kissinger, Simon Perdrix & John van de Wetering (2020): *Graph-theoretic Simplification of Quantum Circuits with the ZX-calculus*.
- [10] Michael H. Freedman, Alexei Kitaev, Michael J. Larsen & Zhenghan Wang (2002): *Topological quantum computation*. *Bulletin of the American Mathematical Society* 40(01), pp. 31–39, doi:10.1090/s0273-0979-02-00964-3. Available at <https://doi.org/10.1090/s0273-0979-02-00964-3>.
- [11] Xiaoyan Gong & Quanlong Wang (2017): *Equivalence of Local Complementation and Euler Decomposition in the Qutrit ZX-calculus*.
- [12] Xiaoyan Gong & Quanlong Wang (2017): *Equivalence of local complementation and Euler decomposition in the qutrit ZX-calculus*. *arXiv preprint arXiv:1704.05955*.
- [13] Johnnie Gray & Stefanos Kourtis (2020): *Hyper-optimized tensor network contraction*.
- [14] Erik Hostens, Jeroen Dehaene & Bart De Moor (2005): *Stabilizer states and Clifford operations for systems of arbitrary dimensions and modular arithmetic*. *Physical Review A* 71(4), doi:10.1103/physreva.71.042315. Available at <http://dx.doi.org/10.1103/PhysRevA.71.042315>.
- [15] F. Jaeger, D. L. Vertigan & D. J. A. Welsh (1990): *On the computational complexity of the Jones and Tutte polynomials*. *Mathematical Proceedings of the Cambridge Philosophical Society* 108(1), p. 35–53, doi:10.1017/S0305004100068936.
- [16] Louis H Kauffman (2001): *Knots and Physics*. WORLD SCIENTIFIC, doi:10.1142/4256. Available at <https://doi.org/10.1142/4256>.

- [17] Greg Kuperberg (2014): *How hard is it to approximate the Jones polynomial?*
- [18] Claire Levaillant, Bela Bauer, Michael Freedman, Zhenghan Wang & Parsa Bonderson (2015): *Universal gates via fusion and measurement operations on $SU(2)$ anyons*. *Physical Review A* 92(1), doi:10.1103/physreva.92.012301. Available at <http://dx.doi.org/10.1103/PhysRevA.92.012301>.
- [19] Konstantinos Meichanetzidis & Stefanos Kourtis (2019): *Evaluating the Jones polynomial with tensor networks*. *Phys. Rev. E* 100, p. 033303, doi:10.1103/PhysRevE.100.033303. Available at <https://link.aps.org/doi/10.1103/PhysRevE.100.033303>.
- [20] Jiannis K. Pachos (2012): *Introduction to Topological Quantum Computation*. Cambridge University Press, doi:10.1017/CBO9780511792908.
- [21] Eric C. Rowell & Zhenghan Wang (2018): *Mathematics of topological quantum computing*. *Bulletin of the American Mathematical Society* 55(2), p. 183–238, doi:10.1090/bull/1605. Available at <http://dx.doi.org/10.1090/BULL/1605>.
- [22] Quanlong Wang (2018): *Qutrit ZX-calculus is Complete for Stabilizer Quantum Mechanics*.
- [23] Quanlong Wang (2020): *Completeness of algebraic ZX-calculus over arbitrary commutative rings and semirings*.
- [24] John van de Wetering (2020): *ZX-calculus for the working quantum computer scientist*.
- [25] Edward Witten (1989): *Quantum field theory and the Jones polynomial*. *Communications in Mathematical Physics* 121(3), pp. 351–399, doi:10.1007/bf01217730. Available at <https://doi.org/10.1007/bf01217730>.
- [26] F. Y. Wu (1992): *Knot theory and statistical mechanics*. *Rev. Mod. Phys.* 64, pp. 1099–1131, doi:10.1103/RevModPhys.64.1099. Available at <https://link.aps.org/doi/10.1103/RevModPhys.64.1099>.

A Qubit ZX Calculus

The well-known rewrite rules of the qubit ZX-calculus are shown in Fig.1.

B Qutrit ZX Calculus

We now give a full set of rules defining the qutrit ZX-calculus. Our presentation aims for clarity and accessibility; for a more rigorous description, see [22].

Definition B.1. The *qutrit ZX-calculus* is a graphical calculus generated by the following diagrams, where $\alpha, \beta \in [0, 2\pi]$:

$$\left\{ \begin{array}{c} \dots \\ \text{---} \circ \text{---} \\ \alpha \\ \beta \\ \text{---} \circ \text{---} \\ \dots \end{array} \right\}, \quad \left\{ \begin{array}{c} \dots \\ \text{---} \circ \text{---} \\ \alpha \\ \beta \\ \text{---} \circ \text{---} \\ \dots \end{array} \right\}, \quad \left\{ \begin{array}{c} | \\ \text{---} \text{---} \\ | \end{array} \right\}, \quad \left\{ \begin{array}{c} \diagup \quad \diagdown \\ \diagdown \quad \diagup \end{array} \right\}, \quad \left\{ \begin{array}{c} | \end{array} \right\} \quad (27)$$

and their adjoints $(-)^{\dagger}$. Adjoints are found by swapping inputs and outputs and negating any decorations - recall negation is mod 2π for general spider phases, and mod 3 for integer spider phases and

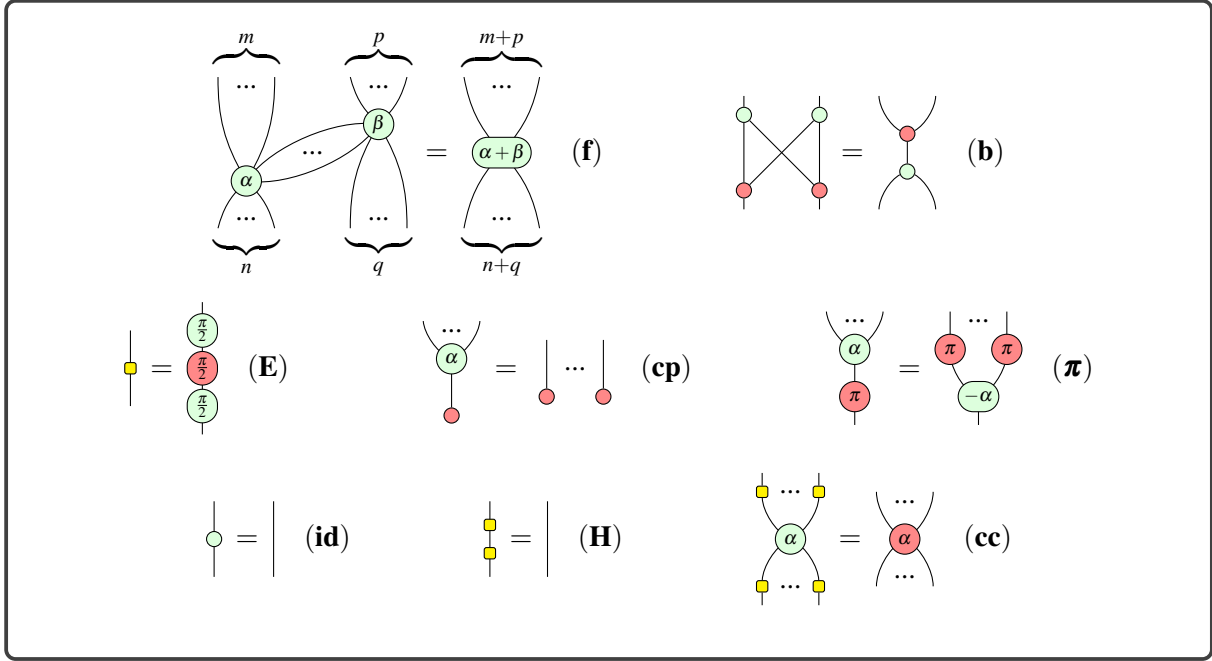


Figure 1: Rewrite rules for the qubit ZX-calculus where spiders are interpreted as tensors over \mathbb{C} .

Hadamard boxes. Thus the two rightmost generators are self-adjoint, whereas the first three satisfy:

$$\left(\begin{array}{c} m \\ \vdots \\ \alpha \\ \beta \\ \vdots \\ n \end{array} \right)^\dagger = \begin{array}{c} n \\ \vdots \\ -\alpha \\ -\beta \\ \vdots \\ m \end{array}, \quad \left(\begin{array}{c} m \\ \vdots \\ \alpha \\ \beta \\ \vdots \\ n \end{array} \right)^\dagger = \begin{array}{c} n \\ \vdots \\ -\alpha \\ -\beta \\ \vdots \\ m \end{array}, \quad \left(\begin{array}{c} 1 \\ \vdots \\ 1 \end{array} \right)^\dagger = \begin{array}{c} 2 \\ \vdots \\ 2 \end{array} \quad (28)$$

These generators can be composed in parallel (\otimes) and sequentially (\circ), and the resulting diagrams are governed by the rewrite rules in Figure 2, wherein addition is modulo 2π . The fusion rule (f) applies to spiders of the same colour connected by at least one wire. Importantly, all the rules hold under taking adjoints, where for diagrams D and E we have:

$$(D \otimes E)^\dagger = D^\dagger \otimes E^\dagger, \quad (D \circ E)^\dagger = D^\dagger \circ E^\dagger \quad (29)$$

Furthermore, it can be derived that all but the commutation equations (cm) and the colour change equations (cc) continue to hold when the roles of green and red (i.e. Z and X) are interchanged. For these four exceptions, however, analogous equations can be derived from the existing ones; for example, the corresponding colour change equations will be relevant for us later.

Proposition B.2. The following equations are derivable in the qutrit ZX-calculus:

$$\begin{array}{c} \vdots \\ \alpha \\ \beta \\ \vdots \end{array} = \begin{array}{c} 1 \quad \vdots \quad 1 \\ \vdots \\ \alpha \\ \beta \\ \vdots \\ 2 \quad \vdots \quad 2 \end{array}, \quad \begin{array}{c} \vdots \\ \beta \\ \alpha \\ \vdots \end{array} = \begin{array}{c} 2 \quad \vdots \quad 2 \\ \vdots \\ \alpha \\ \beta \\ \vdots \\ 1 \quad \vdots \quad 1 \end{array} \quad (30)$$

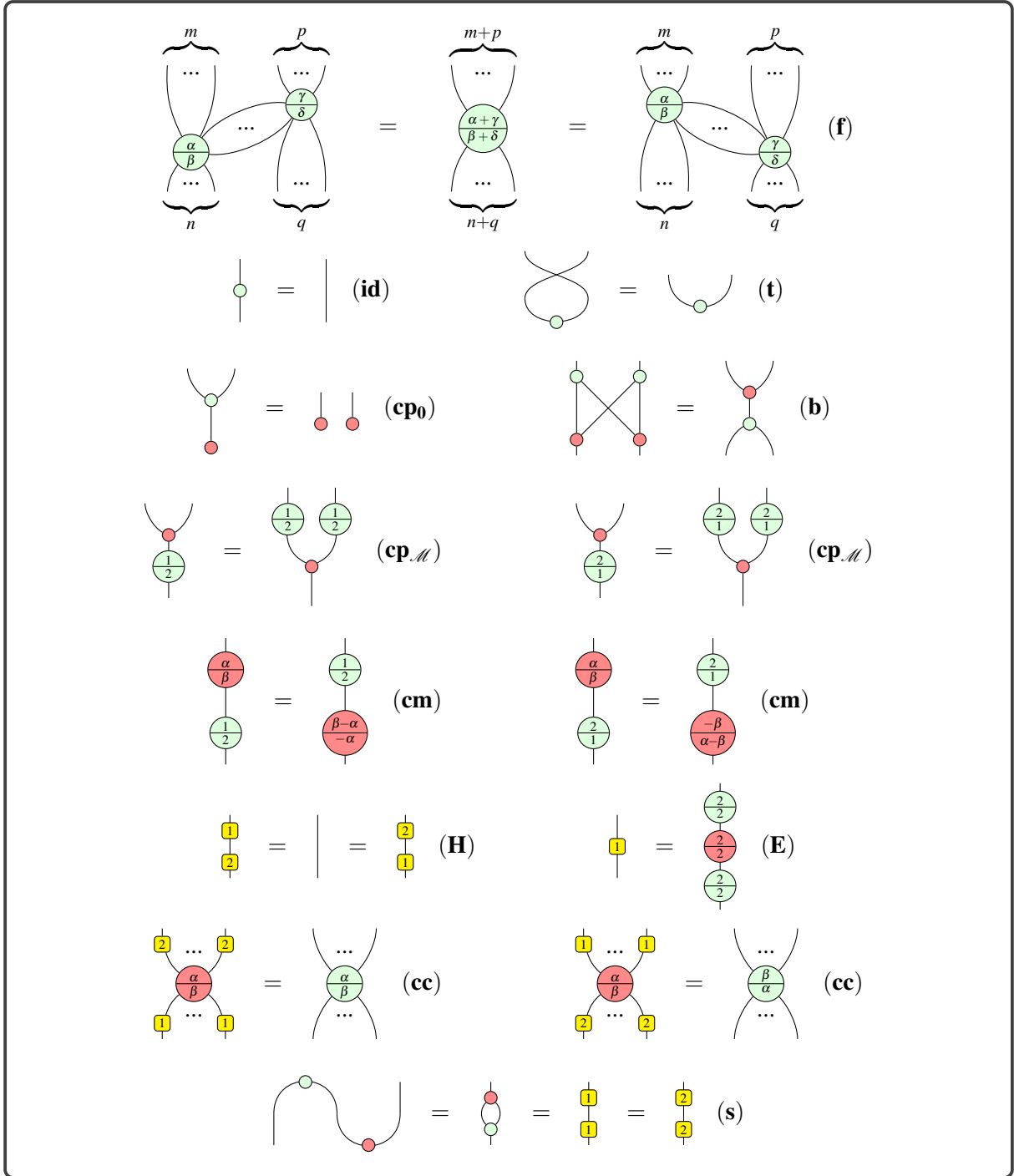


Figure 2: Rewrite rules for the qutrit ZX-calculus where spiders are interpreted as tensors over \mathbb{C} .

Proof. Add H - and H^\dagger -boxes to both sides of the original colour change equations in such a way that we can then cancel Hadamards on the legs of the red spiders via **(H)**. \square

Lemma B.3. The following equations hold in the qutrit ZX-calculus:

$$(31)$$

Proof. It is shown in Lemma 2.8 [11] that the qutrit ZX-calculus satisfies the following ‘Hopf law’:

$$(32)$$

Therefore, to prove the first equation, we can argue as follows, for $h \in \{1, 2\}$:

$$(33)$$

The other two equations are proved in (Lemma 3.4, [12]). \square

C Pivoting in the Qutrit ZX-Calculus

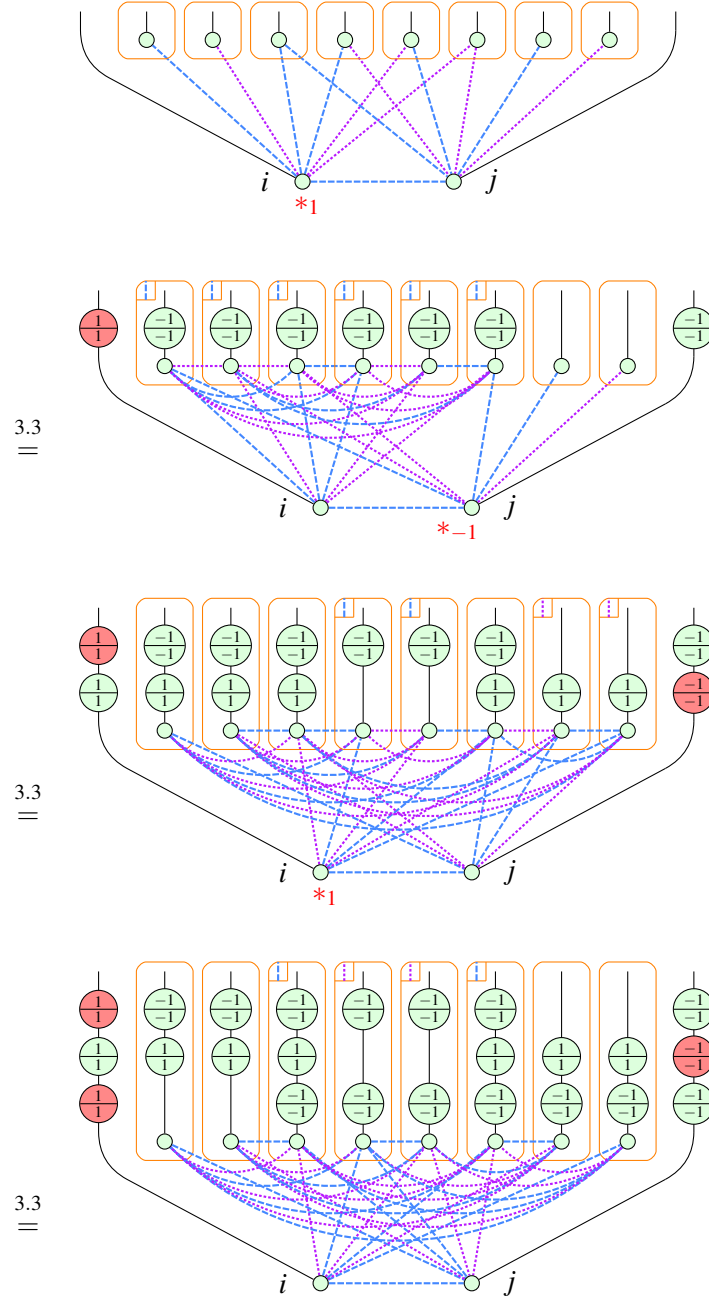
Next we prove the pivot equality from Theorem 3.5. We require the following: since **(E)** holds under taking adjoints, and swapping the roles of red and green, we have:

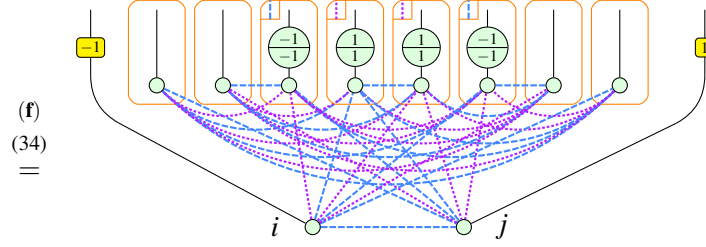
$$(34)$$

Theorem C.1. / Theorem 3.5. Given $a \in \mathbb{Z}_3$ and a graph state (G, W) containing connected nodes i and j , define $N_=(i, j) := \{x \in N(i) \cap N(j) \mid w_{x,i} = w_{x,j}\}$ and $N_\neq(i, j) := \{x \in N(i) \cap N(j) \mid w_{x,i} \neq w_{x,j}\}$. Then the following equation relates G and its proper a -pivot along ij :

$$(35)$$

Proof. There are four cases $(a, w_{i,j} \in \{1, 2\})$, which split into two pairs of symmetric cases: $a = w_{i,j}$ and $a \neq w_{i,j}$. We show just one case - the 1-pivot along ij of weight 1 - the remaining cases being analogous. We again employ the !-notation. An asterisk $*_a$ next to a spider means that at the next step an a -local complementation will be performed at this spider.





□

D Spider Elimination Rules for Qutrit ZX

Now we prove the three elimination theorems for \mathcal{P} -, \mathcal{N} - and \mathcal{M} -spiders. All three require the following two lemmas.

Lemma D.1. The following ‘leg flip’ equation holds in the qutrit ZX-calculus:

(36)

Proof.

(37)

□

Lemma D.2. The following more substantial ‘ \mathcal{M} -copy’ rule holds in the qutrit ZX-calculus, for any \mathcal{M} -spider state (i.e. $m \in \{0, 1, 2\}$ below):

(38)

Proof. First we prove that an \mathcal{M} -spider with non-trivial phase (i.e. $m \in \{1, 2\}$) satisfies a copy rule exactly like the rule (**cp**₀):

(39)

[illegible]
$$\begin{array}{c} \dots \\ | \\ \textcircled{\alpha/\beta} \\ | \\ \textcircled{m/-m} \end{array} \quad (\mathbf{f}) = \begin{array}{c} \dots \\ | \\ \textcircled{} \\ / \quad | \quad \backslash \\ \textcircled{\alpha/\beta} \quad \textcircled{m/-m} \quad \textcircled{m/-m} \end{array} \quad (40) = \begin{array}{c} | \quad \dots \quad | \\ | \quad \quad \quad | \\ \textcircled{m/-m} \quad \textcircled{m/-m} \quad \textcircled{\alpha/\beta} \quad \textcircled{m/-m} \quad \textcircled{m/-m} \end{array} = \begin{array}{c} | \quad \dots \quad | \\ | \quad \quad \quad | \\ \textcircled{m/-m} \quad \textcircled{m/-m} \quad \textcircled{m/-m} \end{array} \quad (41)$$

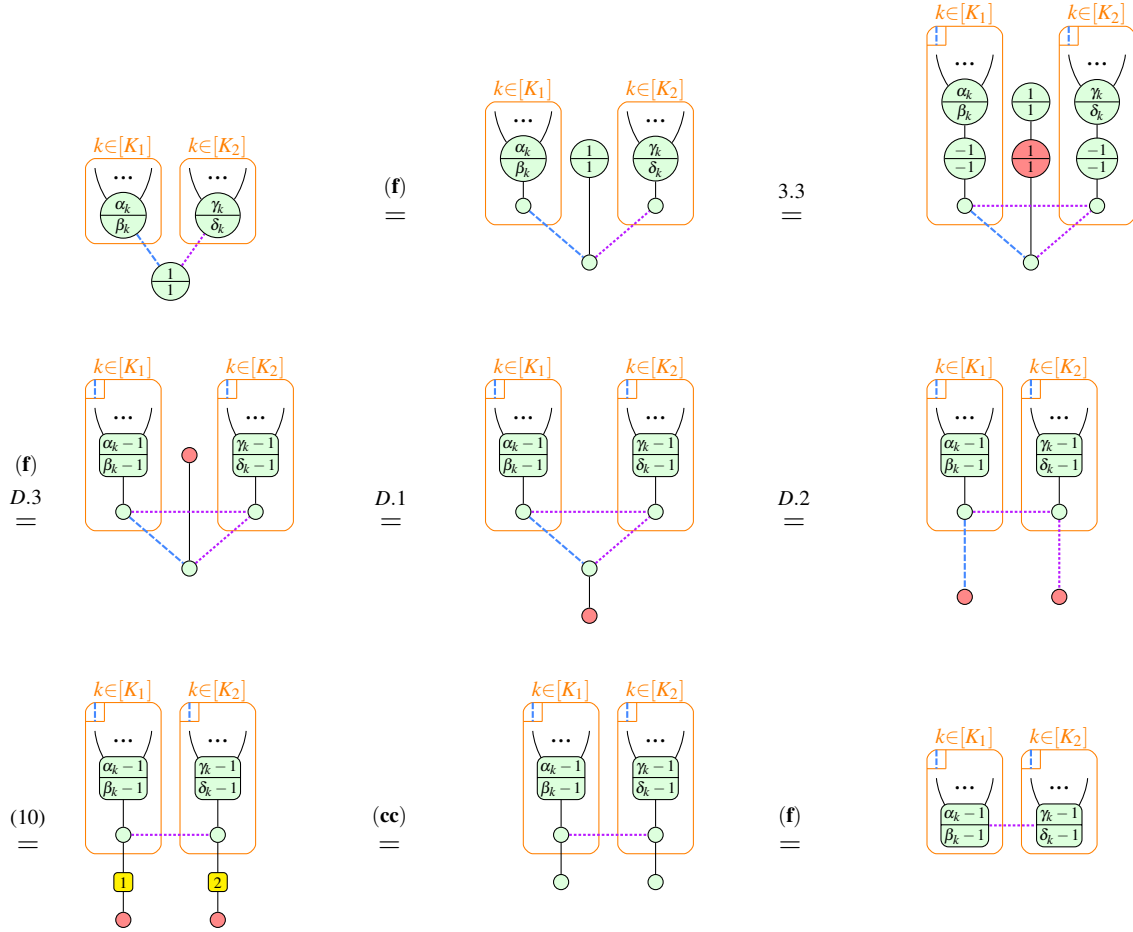
The \mathcal{P} -spider elimination theorem additionally requires a lemma allowing us to turn a \mathcal{P} -spider state of one colour into a \mathcal{P} -spider state of the other. We will use this lemma its adjoint form in the proof of the main theorem.

$$\begin{array}{c} | \\ \textcircled{p} \\ \hline \textcircled{p} \end{array} = \begin{array}{c} | \\ \textcircled{-p} \\ \hline \textcircled{-p} \end{array} \quad (42)$$
$$\begin{array}{c} | \\ \circlearrowleft \frac{p}{p} \\ | \end{array} \stackrel{(\text{cc})}{=} \begin{array}{c} | \\ \textcolor{yellow}{\circ} p \\ | \end{array} \stackrel{(34)}{=} \begin{array}{c} | \\ \circlearrowleft \frac{-p}{-p} \\ | \end{array} \stackrel{(\text{f})}{=} \begin{array}{c} | \\ \circlearrowleft \frac{-p}{-p} \\ | \end{array} \stackrel{D.2}{=} \begin{array}{c} | \\ \circlearrowleft \frac{-p}{-p} \\ | \end{array} \stackrel{(\text{f})}{=} \begin{array}{c} | \\ \circlearrowleft \frac{-p}{-p} \\ | \end{array} \stackrel{(\text{f})}{=} \begin{array}{c} | \\ \circlearrowleft \frac{-p}{-p} \\ | \end{array} \quad (43)$$

9

The diagram shows the decomposition of a joint distribution into a product of marginal distributions and a conditional distribution. On the left, a joint distribution is represented by a green circle containing α_k and β_k , and another green circle containing γ_k and δ_k . These are connected by a blue dashed line labeled $\frac{p}{p}$. The right side shows the same joint distribution as a product of two marginal distributions (green circles) and a conditional distribution (yellow circle). The first marginal distribution contains α_k and β_k , the second contains γ_k and δ_k , and the conditional distribution contains $\frac{p}{p}$. The marginal distributions are labeled $k \in [K_1]$ and $k \in [K_2]$ respectively.

Proof. For clarity of presentation we only show the case $\frac{p}{p} = \frac{1}{1}$, the other case being near-identical.



□

D.2 \mathcal{N} -spider Elimination

Proving the corresponding \mathcal{N} -spider elimination theorem again requires a lemma allowing us to turn an \mathcal{N} -spider state of one colour into an \mathcal{N} -spider state of the other.

Lemma D.5. The following rules hold in the qutrit ZX-calculus:

$$\begin{array}{c} 0 \\ 1 \end{array} = \begin{array}{c} 2 \\ 0 \end{array}, \quad \begin{array}{c} 0 \\ 2 \end{array} = \begin{array}{c} 0 \\ 1 \end{array}, \quad \begin{array}{c} 1 \\ 0 \end{array} = \begin{array}{c} 0 \\ 2 \end{array}, \quad \begin{array}{c} 2 \\ 0 \end{array} = \begin{array}{c} 1 \\ 0 \end{array} \quad (44)$$

Proof. For any green \mathcal{N} -spider state with phase $\frac{n}{n'}$, we have a choice of two colour change rules which we could use to turn it into a red \mathcal{N} -spider state with a H - or H^\dagger -box on top:

$$\begin{array}{c} 2 \\ n \\ n' \end{array} \stackrel{(cc)}{=} \begin{array}{c} n \\ n' \end{array} \stackrel{(cc)}{=} \begin{array}{c} 1 \\ n' \\ n \end{array} \quad (45)$$

Of these two choices, exactly one has a decomposition of the H -/ H^\dagger -box as in (34) that allows the bottom two red spiders to fuse into an \mathcal{M} -spider, which we can then move past the green spider above it via D.2. For brevity we only show the case $\begin{smallmatrix} n \\ 1 \end{smallmatrix} = \begin{smallmatrix} 0 \\ 1 \end{smallmatrix}$:

$$\begin{array}{c} \begin{smallmatrix} 0 \\ 1 \end{smallmatrix} \end{array} \stackrel{\text{(cc)}}{=} \begin{array}{c} \begin{smallmatrix} 2 \\ 1 \end{smallmatrix} \end{array} \stackrel{(34)}{=} \begin{array}{c} \begin{smallmatrix} 1 \\ 1 \end{smallmatrix} \\ \begin{smallmatrix} 1 \\ 1 \end{smallmatrix} \\ \begin{smallmatrix} 1 \\ 1 \end{smallmatrix} \\ \begin{smallmatrix} 0 \\ 1 \end{smallmatrix} \end{array} \stackrel{\text{(f)}}{=} \begin{array}{c} \begin{smallmatrix} 1 \\ 1 \end{smallmatrix} \\ \begin{smallmatrix} 1 \\ 1 \end{smallmatrix} \\ \begin{smallmatrix} 1 \\ 2 \end{smallmatrix} \end{array} \stackrel{D.2}{=} \begin{array}{c} \begin{smallmatrix} 1 \\ 1 \end{smallmatrix} \\ \begin{smallmatrix} 1 \\ 2 \end{smallmatrix} \end{array} \stackrel{\text{(f)}}{=} \begin{array}{c} \begin{smallmatrix} 2 \\ 0 \end{smallmatrix} \end{array} \quad (46)$$

□

Corollary D.6. The following equations hold in the qutrit ZX-calculus, for $n \in \{1, 2\}$:

$$\begin{array}{c} \begin{smallmatrix} 0 \\ n \end{smallmatrix} \\ \begin{smallmatrix} -n \\ -n \end{smallmatrix} \end{array} = \begin{array}{c} \begin{smallmatrix} 2 \\ 1 \end{smallmatrix} \end{array}, \quad \begin{array}{c} \begin{smallmatrix} n \\ 0 \end{smallmatrix} \\ \begin{smallmatrix} -n \\ -n \end{smallmatrix} \end{array} = \begin{array}{c} \begin{smallmatrix} 1 \\ 2 \end{smallmatrix} \end{array} \quad (47)$$

Proof. Again we only prove one case, the other three being analogous. Each case uses D.5 in its adjoint form - recall that the adjoint of a spider is found by swapping inputs and outputs and negating angles.

$$\begin{array}{c} \begin{smallmatrix} 0 \\ 1 \end{smallmatrix} \\ \begin{smallmatrix} -1 \\ -1 \end{smallmatrix} \end{array} = \begin{array}{c} \begin{smallmatrix} 0 \\ -2 \end{smallmatrix} \\ \begin{smallmatrix} -1 \\ -1 \end{smallmatrix} \end{array} \stackrel{D.5}{=} \begin{array}{c} \begin{smallmatrix} 0 \\ -1 \end{smallmatrix} \\ \begin{smallmatrix} -1 \\ -1 \end{smallmatrix} \end{array} \stackrel{\text{(f)}}{=} \begin{array}{c} \begin{smallmatrix} -1 \\ -2 \end{smallmatrix} \end{array} = \begin{array}{c} \begin{smallmatrix} 2 \\ 1 \end{smallmatrix} \end{array} \quad (48)$$

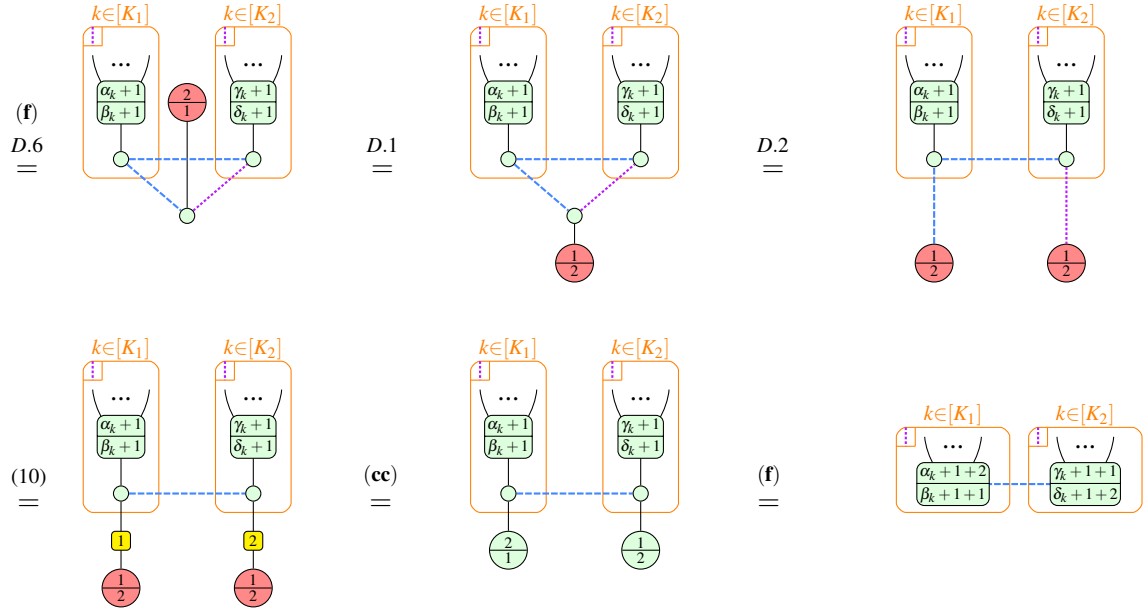
□

Theorem D.7. / Theorem 3.7. Given any graph-like ZX-diagram containing an interior \mathcal{N} -spider x with phase $\begin{smallmatrix} 0 \\ n \end{smallmatrix}$ or $\begin{smallmatrix} n \\ 0 \end{smallmatrix}$ for $n \in \{1, 2\}$, suppose we perform a $(-n)$ -local complementation at x . Then, treating the two cases separately, the new ZX-diagrams are related to the old ones by the equalities:

$$\begin{array}{c} \begin{array}{c} k \in [K_1] \quad k \in [K_2] \\ \dots \quad \dots \\ \alpha_k \quad \gamma_k \\ \beta_k \quad \delta_k \\ \begin{smallmatrix} 0 \\ n \end{smallmatrix} \end{array} \end{array} = \begin{array}{c} \begin{array}{c} k \in [K_1] \quad k \in [K_2] \\ \dots \quad \dots \\ \alpha_k + n + 2 \quad \gamma_k + n + 1 \\ \beta_k + n + 1 \quad \delta_k + n + 2 \\ \begin{smallmatrix} -n \end{smallmatrix} \end{array} \end{array}, \quad \begin{array}{c} \begin{array}{c} k \in [K_1] \quad k \in [K_2] \\ \dots \quad \dots \\ \alpha_k \quad \gamma_k \\ \beta_k \quad \delta_k \\ \begin{smallmatrix} n \\ 0 \end{smallmatrix} \end{array} \end{array} = \begin{array}{c} \begin{array}{c} k \in [K_1] \quad k \in [K_2] \\ \dots \quad \dots \\ \alpha_k + n + 1 \quad \gamma_k + n + 2 \\ \beta_k + n + 2 \quad \delta_k + n + 1 \\ \begin{smallmatrix} -n \end{smallmatrix} \end{array} \end{array}$$

Proof. We prove the case where x has phase $\begin{smallmatrix} 0 \\ 1 \end{smallmatrix}$, the other cases being near-identical.

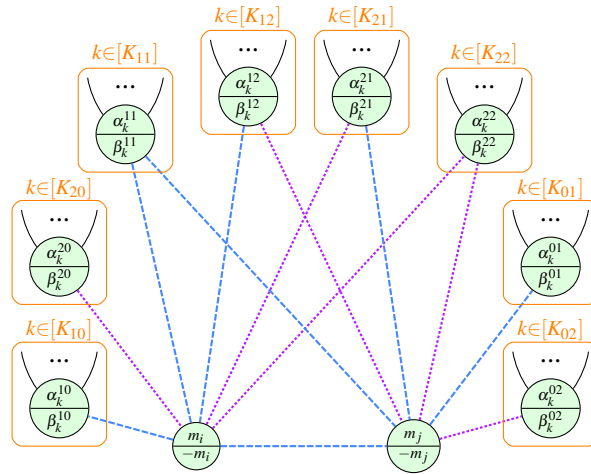
$$\begin{array}{c} \begin{array}{c} k \in [K_1] \quad k \in [K_2] \\ \dots \quad \dots \\ \alpha_k \quad \gamma_k \\ \beta_k \quad \delta_k \\ \begin{smallmatrix} 0 \\ 1 \end{smallmatrix} \end{array} \end{array} \stackrel{\text{(f)}}{=} \begin{array}{c} \begin{array}{c} k \in [K_1] \quad k \in [K_2] \\ \dots \quad \dots \\ \alpha_k \quad \gamma_k \\ \beta_k \quad \delta_k \\ \begin{smallmatrix} 0 \\ 1 \end{smallmatrix} \end{array} \end{array} \stackrel{3.3}{=} \begin{array}{c} \begin{array}{c} k \in [K_1] \quad k \in [K_2] \\ \dots \quad \dots \\ \alpha_k \quad \gamma_k \\ \beta_k \quad \delta_k \\ \begin{smallmatrix} 0 \\ 1 \end{smallmatrix} \end{array} \end{array}$$

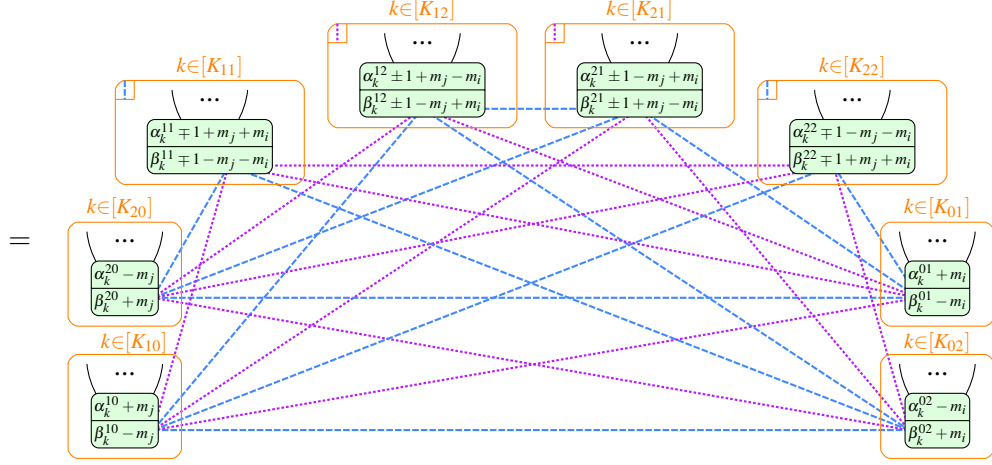


□

D.3 \mathcal{M} -spider Elimination

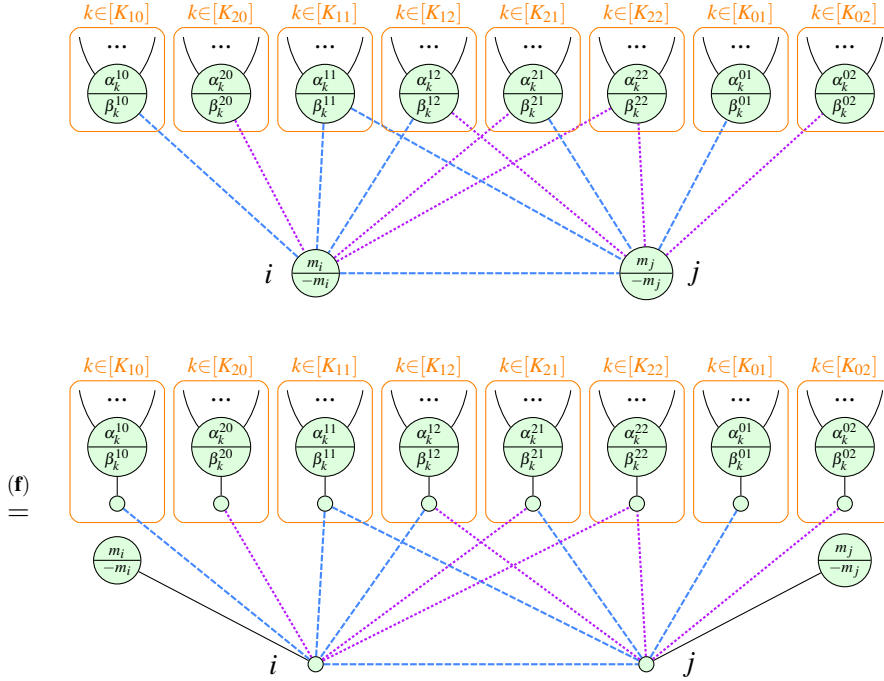
Theorem D.8. / Theorem 3.8. Given any graph-like ZX-diagram containing two interior \mathcal{M} -spiders i and j connected by edge ij of weight $w_{i,j} =: w \in \{1, 2\}$, suppose we perform a proper $\pm w$ -pivot along ij (both choices give the same result). For the case $w = 1$, the new ZX-diagram is related to the old one by the following equality:

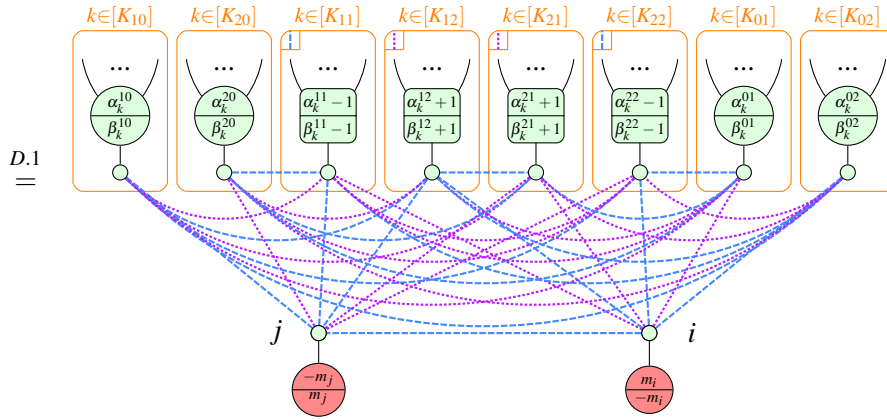
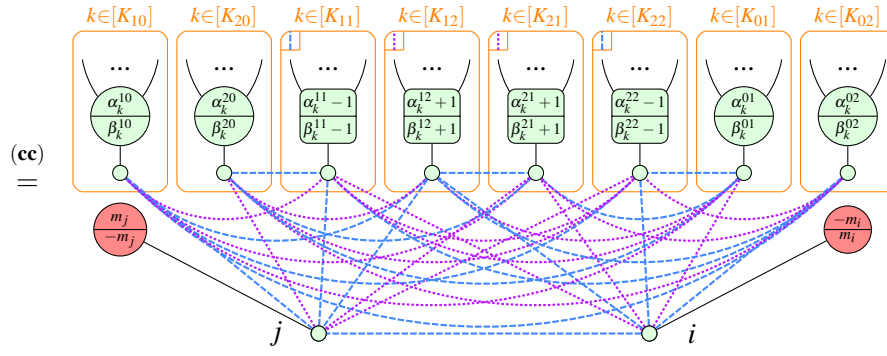
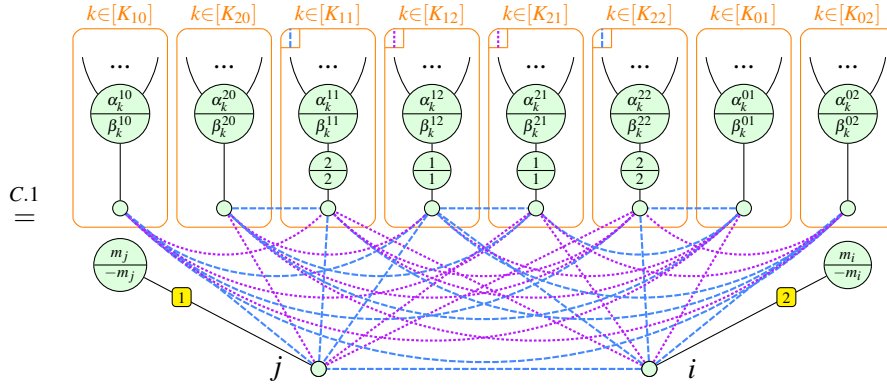


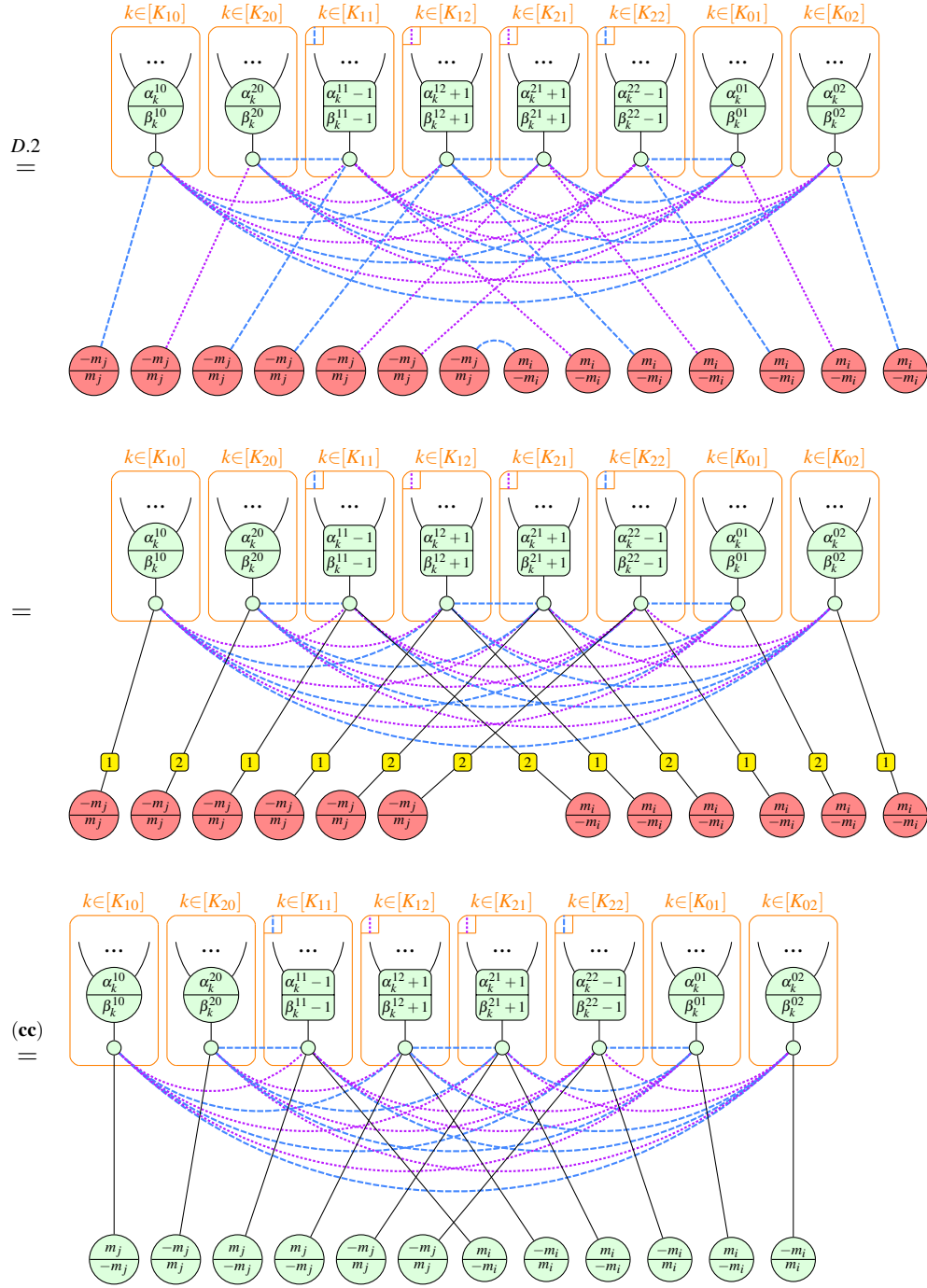


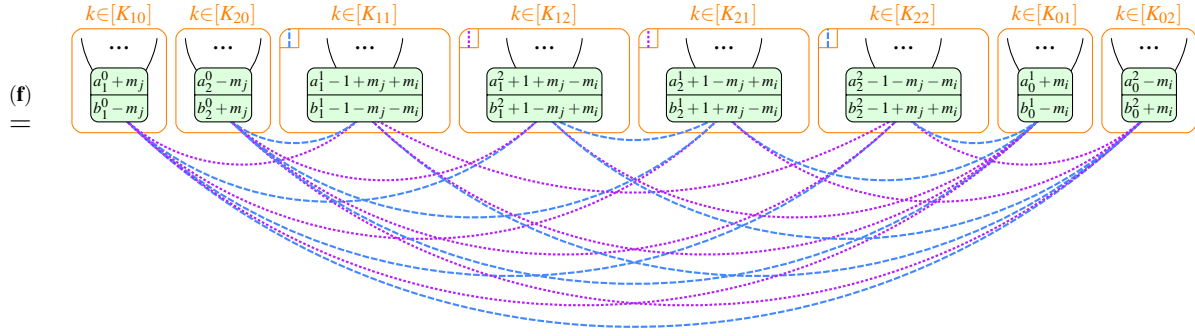
The case $w = 2$ differs only as follows: in the first diagram (the left hand side of the equation), the edge ij is purple (by definition), while in the lower diagram (the right hand side of the equation), a $\pm 2 = \mp 1$ will replace all occurrences of ± 1 , and the roles of purple and blue will be swapped throughout.

Proof. We show the case where $w_{ij} =: w = 1$, with the case $w = 2$ being completely analogous. We can choose either a proper 1-pivot or a proper 2-pivot; both give the same result. Here we only show the former:









□

E \pm -Boxes in the ZX Calculus

We close by proving that the \pm -boxes in (22) correspond to stabilizer ZX-diagrams.

Proposition E.1. The following equalities hold up to a scalar under the standard interpretation:

$$\left[\begin{array}{c} \boxed{\pm} \\ | \end{array} \right]_{d=2} \simeq \left[\begin{array}{c} \text{red circle with } \pm \frac{\pi}{2} \\ | \end{array} \right], \quad \left[\begin{array}{c} \boxed{\pm} \\ | \end{array} \right]_{d=3} \simeq \left[\begin{array}{c} \text{red circle with } \pm \frac{\pi}{2} \\ | \end{array} \right], \quad \left[\begin{array}{c} \boxed{\pm} \\ | \end{array} \right]_{d=4} \simeq \left[\begin{array}{c} \pi \text{ --- } \text{yellow box} \text{ --- } \pi \\ | \end{array} \right] \quad (49)$$

Proof. Recalling $\omega = e^{i\frac{2\pi}{3}}$, the standard interpretations of phase gates in matrix form are:

$$\left[\begin{array}{c} \text{green circle with } \alpha \\ | \end{array} \right] = \begin{pmatrix} 1 & 0 \\ 0 & e^{i\alpha} \end{pmatrix}, \quad \left[\begin{array}{c} \text{red circle with } \alpha \\ | \end{array} \right] = \frac{1}{2} \begin{pmatrix} 1 + e^{i\alpha} & 1 - e^{i\alpha} \\ 1 - e^{i\alpha} & 1 + e^{i\alpha} \end{pmatrix}, \quad \left[\begin{array}{c} \text{green circle with } \frac{\alpha}{\beta} \\ | \end{array} \right] = \begin{pmatrix} 1 & 0 & 0 \\ 0 & e^{i\alpha} & 0 \\ 0 & 0 & e^{i\beta} \end{pmatrix}$$

$$\left[\begin{array}{c} \text{red circle with } \frac{\alpha}{\beta} \\ | \end{array} \right] = \frac{1}{3} \begin{pmatrix} 1 + e^{i\alpha} + e^{i\beta} & 1 + \bar{\omega}e^{i\alpha} + \omega e^{i\beta} & 1 + \omega e^{i\alpha} + \bar{\omega}e^{i\beta} \\ 1 + \omega e^{i\alpha} + \bar{\omega}e^{i\beta} & 1 + e^{i\alpha} + e^{i\beta} & 1 + \bar{\omega}e^{i\alpha} + \omega e^{i\beta} \\ 1 + \bar{\omega}e^{i\alpha} + \omega e^{i\beta} & 1 + \omega e^{i\alpha} + \bar{\omega}e^{i\beta} & 1 + e^{i\alpha} + e^{i\beta} \end{pmatrix}$$

So in the simplest case $d = 2$ it is fairly straightforward to see that:

$$\left[\begin{array}{c} \text{red circle with } \pm \frac{\pi}{2} \\ | \end{array} \right] = \frac{1}{2} \begin{pmatrix} 1 \pm i & 1 \mp i \\ 1 \mp i & 1 \pm i \end{pmatrix} = \frac{\sqrt{2}}{2} e^{\mp i\frac{\pi}{4}} \begin{pmatrix} \pm i & 1 \\ 1 & \pm i \end{pmatrix} = \frac{\sqrt{2}}{2} e^{\mp i\frac{\pi}{4}} \left[\begin{array}{c} \boxed{\pm} \\ | \end{array} \right]_{d=2} \quad (50)$$

The next case $d = 3$ is proved similarly:

$$\begin{aligned}
 \left[\begin{array}{c} \text{red circle with } \pm 1 \\ \text{red circle with } \pm 1 \end{array} \right] &= \frac{1}{3} \begin{pmatrix} 1 + e^{\pm i \frac{2\pi}{3}} + e^{\pm i \frac{2\pi}{3}} & 1 + \bar{\omega} e^{\pm i \frac{2\pi}{3}} + \omega e^{\pm i \frac{2\pi}{3}} & 1 + \omega e^{\pm i \frac{2\pi}{3}} + \bar{\omega} e^{\pm i \frac{2\pi}{3}} \\ 1 + \omega e^{\pm i \frac{2\pi}{3}} + \bar{\omega} e^{\pm i \frac{2\pi}{3}} & 1 + e^{\pm i \frac{2\pi}{3}} + e^{\pm i \frac{2\pi}{3}} & 1 + \bar{\omega} e^{\pm i \frac{2\pi}{3}} + \omega e^{\pm i \frac{2\pi}{3}} \\ 1 + \bar{\omega} e^{\pm i \frac{2\pi}{3}} + \omega e^{\pm i \frac{2\pi}{3}} & 1 + \omega e^{\pm i \frac{2\pi}{3}} + \bar{\omega} e^{\pm i \frac{2\pi}{3}} & 1 + e^{\pm i \frac{2\pi}{3}} + e^{\pm i \frac{2\pi}{3}} \end{pmatrix} \\
 &= \frac{1}{3} \begin{pmatrix} \sqrt{3} e^{\pm i \frac{\pi}{2}} & \sqrt{3} e^{\mp i \frac{\pi}{6}} & \sqrt{3} e^{\mp i \frac{\pi}{6}} \\ \sqrt{3} e^{\mp i \frac{\pi}{6}} & \sqrt{3} e^{\pm i \frac{\pi}{2}} & \sqrt{3} e^{\mp i \frac{\pi}{6}} \\ \sqrt{3} e^{\mp i \frac{\pi}{6}} & \sqrt{3} e^{\mp i \frac{\pi}{6}} & \sqrt{3} e^{\pm i \frac{\pi}{2}} \end{pmatrix} \\
 &= \frac{\sqrt{3}}{3} e^{\mp i \frac{\pi}{6}} \begin{pmatrix} e^{\pm i \frac{2\pi}{3}} & 1 & 1 \\ 1 & e^{\pm i \frac{2\pi}{3}} & 1 \\ 1 & 1 & e^{\pm i \frac{2\pi}{3}} \end{pmatrix} \\
 &= \frac{\sqrt{3}}{3} e^{\mp i \frac{\pi}{6}} \left[\begin{array}{c} \text{box with } \pm \\ \text{box with } \pm \end{array} \right]_{d=3}
 \end{aligned} \tag{51}$$

For the other qubit case $d = 4$ we first note:

$$\left[\begin{array}{c} \text{yellow square} \\ \text{yellow square} \end{array} \right] = \left[\begin{array}{c} \text{green circle with } \frac{\pi}{2} \\ \text{red circle with } \frac{\pi}{2} \\ \text{green circle with } \frac{\pi}{2} \end{array} \right] = \left[\begin{array}{c} \text{green circle with } \frac{\pi}{2} \end{array} \right] \left[\begin{array}{c} \text{red circle with } \frac{\pi}{2} \end{array} \right] \left[\begin{array}{c} \text{green circle with } \frac{\pi}{2} \end{array} \right] = \frac{1}{2\sqrt{2}} \begin{pmatrix} 1 & 1 \\ 1 & -1 \end{pmatrix} \tag{52}$$

Then using the standard interpretation for spiders as in (2), we decompose the diagram in such a way that we can apply the standard interpretation:

$$\begin{aligned}
 \left[\begin{array}{c} \text{red circle with } \pi \\ \text{yellow square} \\ \text{red circle with } \pi \end{array} \right] &= \left[\begin{array}{c} \text{diagram with two red circles and a yellow square connected by arcs} \end{array} \right] \\
 &= \left(\left[\begin{array}{c} \text{red circle with } \pi \end{array} \right] \otimes \left[\begin{array}{c} \text{red circle with } \pi \end{array} \right] \right) \left(\left[\begin{array}{c} \text{red circle with } \pi \end{array} \right] \otimes \left[\begin{array}{c} \text{yellow square} \end{array} \right] \otimes \left[\begin{array}{c} \text{red circle with } \pi \end{array} \right] \right) \left(\left[\begin{array}{c} \text{red circle with } \pi \end{array} \right] \otimes \left[\begin{array}{c} \text{red circle with } \pi \end{array} \right] \right) \\
 &= \frac{\sqrt{2}}{8} \begin{pmatrix} -1 & 1 & 1 & 1 \\ 1 & -1 & 1 & 1 \\ 1 & 1 & -1 & 1 \\ 1 & 1 & 1 & -1 \end{pmatrix} \\
 &= \frac{\sqrt{2}}{8} \left[\begin{array}{c} \text{box with } \pm \\ \text{box with } \pm \end{array} \right]_{d=4}
 \end{aligned}$$

□